

**HIGH IMPEDANCE FAULT DETECTION USING
DISCRETE WAVELET TRANSFORM FOR
TRANSMISSION AND DISTRIBUTION SMART GRIDS**

A Project Report Submitted in partial fulfillment of
the requirements for the award of the degree of

DUAL DEGREE-B.TECH & M.TECH
In
ELECTRICAL ENGINEERING
With VLSI Design and Microelectronics

by
T. Ajay Rama Murthy (EE09B062)

Under the guidance of
Dr. K. Shanti Swarup



**DEPARTMENT OF ELECTRICAL ENGINEERING
INDIAN INSTITUTE OF TECHNOLOGY MADRAS
CHENNAI - 600036
MAY - 2014**

CERTIFICATE

This is to certify that the project report entitled “**Distributed Artificial Intelligence For Fault Detection In Smart Grids**” submitted by **Mr. T. Ajay Ramamurthy (EE09b062)** is a bonafide record of work carried out by him at Power Systems Laboratory, Department of Electrical Engineering, Indian Institute of Technology Madras, in partial fulfillment for the award of degree of **Dual Degree (B.Tech & M.Tech) in Electrical Engineering with VLSI Design and Microelectronics**

The contents of this report have not been submitted and will not be submitted to any other Institute or University for the award of any degree or diploma.

Dr. K. SHANTI SWARUP

Associate Professor
Power Systems Laboratory
Department of Electrical Engineering
Indian Institute of Technology Madras
Chennai – 600036

Date:

CONTENTS

LIST OF FIGURES.....	5
ACKNOWLEDGEMENT.....	6
ABSTRACT.....	7
CHAPTER 1: INTRODUCTION.....	9
1.1 Motivation	10
1.2 Background.....	11
1.3 Problem Statement.....	12
1.4 Organization of thesis.....	13
CHAPTER 2: HIF AND FAULT ANALYSIS	14
2.1 Fault Analysis	14
2.2 Wavelet Transform.....	18
2.3 Short Time Fourier Transform (DSTFT) method.....	19
2.4 Discrete Wavelet Transform (DWT) method.....	20
2.5 Energy Spectrum of Detail Coefficients.....	28
CHAPTER 3: PROBLEM FORMULATION and SOLUTION METHODOLOGY.....	30
3.1 Problem Statement	30
3.2 Solution methodology.....	31
CHAPTER 4: CASE STUDY WSCC 9-BUS system.....	32
4.1 Single line diagram.....	32
4.2 Simulink Model.....	
4.3 Load Flow data	
CHAPTER 5: SIMULATION AND RESULTS.....	38
5.1 Simulation Conditions.....	38.

5.2 Simulation Results.....	
5. DWT Filter Bank HDL Simulation.....	
CHAPTER 6: CONCLUSION AND FUTURE WORK.....	50
APPENDIX.....	52
REFERENCES.....	54

LIST OF FIGURES

1. Figure 1.0 Power Generation, Transmission, Distribution.....	11
2. Fig. 1.1 DWT filter bank framework.....	12
3. Fig 1.2 Process flow for HIF detection	13
4. Figure 2.1 Fault Classification.....	15
5. Figure 2.2 HIF Model used for simulations of fault characteristics.....	15
6. Figure 2.3 Typical HIF current characteristics.....	16
7. Figure 2.4 : Three-phase circuit diagram of a Phase A-to-B, LL fault.....	16
8. Figure 2.5 : Three-phase circuit diagram of a Phase A-to-B-to-G, LLG fault.....	17
9. Figure 2.6 STWT-DWT windows.....	18
10. Figure 2.7: Schematic of DWT Multi-Resolution Analysis decomposition.....	24
11. Figure 2.8 Scaling, Wavelet functions and Filter coefficients for DB4 wavelet.....	25
12. Figure 2.9 Scaling, Wavelet functions and Filter coefficients for DB6 Wavelet.....	26
13. Figure 2.10 Different Decomposition Scales of Db Wavelet of a signal.....	26
14. Figure 2.11 and 2.12 showing fast rising transients indicating HIF fault for some test system.....	27
15. Fig 2.13 One-line diagram of an example radial distribution feeder.....	28
16. Figure 2.14 HIF Current Waveform, D1 Coefficients and its Detection.....	28
17. Figure 3.1 HIF time varying non-linear resistor model.....	29
18. Figure 4.1 WSCC 9-BUS 3-GENERATOR single line diagram in PSAT	32
19. Figure:4.2 WSCC(Western State Coordinating Council) 9-BUS 3-GENERATOR Test system in SIMULINK.....	35
20. Figure 4.3 Voltage in per unit at different buses.....	36
21. Figure 4.4, Voltage in KV at different buses.....	36
22. Figure 4.5, Voltage phase in rad at different buses.....	36
23. Figure 4.6 Active power at different buses.....	36
24. Figure 4.7 Reactive power at different buses.....	36
25. Figure 5.1 WSCC 9 BUS test system simulink model.....	37
26. figure 5.2 I-V AT BUS_7.....	37

ACKNOWLEDGEMENT

I am deeply indebted to my guide Dr. K Shanti Swarup for allowing me to work on this project. I would like to thank him sincerely for allowing me to learn and explore my areas of interests for this project and for being so patient during the research process and project work . This experience has deepened my knowledge significantly and further increased my enthusiasm to work in the vast field of Electrical Engineering.

Furthermore I would like to thank my professors and friends for their valuable inputs and suggestions

Lastly I would like to thank my family for their unconditional love and immense support which have helped a lot in carrying out this project.

ABSTRACT

Electrical Power Engineering is a multi-disciplinary field as there are numerous applications of different subjects. It can be broadly categorized as power generation, transmission and distribution. There are vast variety of application sub-domains and problems in these sub-domains which give ample scope for using faster optimized methods and techniques in grids making them even more smarter.

A high impedance fault in power system networks results when a primary conductor makes unwanted electrical contact with a road surface, sidewalk, sod, tree limb, or with some other surface, or object which restricts the flow of fault current to a level below that reliably detectable by conventional over-current devices. Often this leaves a conductor energized on the ground surface posing a danger to the public.

The project's focus is mainly on High Impedance Faults (HIF) detections in modern power systems using Discrete Wavelet Transform(DWT) algorithm .The work done is related to DWT signal processing technique being used for real-time applications in Modern power systems by Intelligent Multi-agent systems for fault detection and identification. Intelligent systems are characterized by ability to map input-output relationships from observed data pairs with hope that this learned mapping would deduce the system response for unknown condition , hence reducing fault detection and maintenance times.

Distributed Systems are increasingly being equipped with intelligent devices such as digital protection devices and advanced metering equipment. These devices generally have an inbuilt processor which impart advanced computation capability to them. With

advanced measurement and computation, faster and improved fault detection, location and identification is possible in large power system networks.

For the above mentioned applications of intelligent systems, **signal processing** is essential and core part of it. Beginning with modeling and simulation of working WSCC 9-Bus System in Simulink following are the processes carried out. Load flow analysis, fault simulation (High impedance faults, Single line to ground, double line to ground, and three lines to ground faults),data acquisition at different buses and points for all 3 phases, sampling, Discrete Wavelet Transform (**DWT**) filtering , mother wavelet selection (Db4, Db6 etc), downscaling ,Multi Resolution Analysis (**MRA**) , Detail Spectral Energy Calculation(**DSE**), Filter banks HDL simulation. The Wavelet , Signal Processing , PSAT toolboxes in MATLAB were some tools studied and used for analyzing the bus and line voltages within the simulated WSCC 9-Bus power system and check for HIF faults. All the models and programs were developed in MATLAB and Simulink. Finally the DWT filters were simulated using Verilog HDL in Xilinx for hardware implementation .

Keywords: DWT, WSCC 9-Bus system, HIF Fault, DSE, Daubechies wavelets , detail coefficients, MRA, Filters, Verilog (HDL)

CHAPTER 1

INTRODUCTION:

Electrical power transmission and distribution systems supply power to dispersed residential customers, commercial and small industrial customers in a safe, reliable and economical fashion. This is achieved by maintaining stable voltage levels, making power factor correction through reactive compensation and offering continuous uninterrupted electric power to meet the demand. Electric power supply interruptions can be planned and unplanned. Planned outages are part of maintenance procedures. However, it is the unplanned outage events which are to be minimized. We will focus our study on detecting and identifying some of those power system faults.

Transmission and Distribution system faults are most commonly single or double phase faults. These faults occur when one or more phases come in contact with one another, the ground, or in some case both. These type of faults are commonly detected by traditional power protection systems like relays and circuit breakers which then isolate the faulty section of the power network till the fault is cleared.

When an energized conductor makes an electrical contact with a surface of high resistive value it results in an over-current which is insufficient (i.e much lower value compared to normal threshold) to trip the conventional protection system devices like the over-current relays or fuses and Circuit Breakers. These particular types of faults are categorized as High Impedance Faults (HIF). This can lead to temporary or permanent service outages. Many types of events including lightning flashover, animals, tree limbs and poor weather conditions, such as high winds, and rain, are common causes of the High Impedance fault (HIF) in power systems.

If these faults are not detected quickly, the population part of power distribution network, become exposed to the risk of electrical shocks .The various system equipment and private household devices are prone to damage as well. Therefore there is a need to detect and clear the high impedance (HIF) fault in a fast and reliable way whenever they occur in the transmission and distribution networks. Use of automation or intelligent systems helps us achieve the above objective and restore power system to normal operating conditions.

1.1 MOTIVATION:

Fault detection and fault diagnosis is of special interest to the electrical power industry and even to the customers connected in the distribution grid. When fault occurs in an electric power system, the effects are often not restricted to the faulty section, but noticeable throughout the whole system. The electric power supply becomes unreliable if faults are not diagnosed as soon as they occur. Thus, the restoration after fault occurrence must be carried out by putting in place a scheme capable of fault detection and diagnosis; thus maintaining system stability, minimizing customer and network damages, as well as economic losses.

Large funds and resources are being employed by different countries for research and development to modernize Electrical Power Grids .Hence, special emphasis has been placed on research in Fault detection, isolation and recovery (FDIR) for power systems .With widespread use of intelligent digital devices equipped with powerful processors capable of fast computing and measuring capabilities across different fields ,currently power system networks are also getting equipped with digital layers (a multi-agent system) in an effort to realize SMART Grids or Future Grids.

A multiple agent system is composed of multiple interacting intelligent agents which are

employed in an environment to solve a common problem like fault detection and fault location in a collective way. It would otherwise be difficult for a monolithic system. Each intelligent device is capable of running fault diagnosing algorithms in real-time environment on measured voltage and current samples from the bus network.

For FDIR several approaches have been pursued which include the Discrete Fourier Transform (DFT), the Short Time Fourier Transform (STFT) , Discrete Wavelet Transform (DWT) and Artificial Neural Networks (ANNs). For this project, fault detection is carried out by DWT as it enables us to analyze transients information in time and frequency domains at the same time.

1.2 BACKGROUND

High Impedance Faults (HIF) in electrical power network lead to lot of transient phenomenon. HIFs on electrical transmission and distribution networks involve arcing and/or nonlinear characteristics of fault impedance which cause cyclical pattern distortions. The objective of most detection schemes is to evaluate the special features in patterns of the voltages and currents in HIFs .Therefore transient analysis is vital for fault detection in power systems. It involves sampling of the real time signals in time, to acquire data for further analysis using many signal processing techniques. Transient analysis has been addressed by certain techniques such as DWT (discrete wavelet transform) and STFT (short time fourier transform) previously and even now.

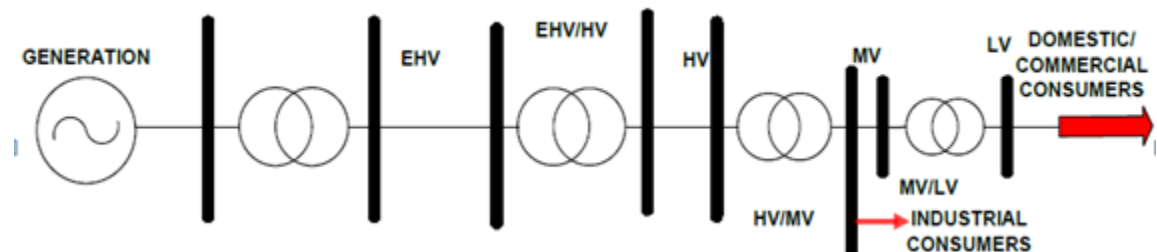


Figure 1.0 Power Generation, Transmission, Distribution network

The DWT is a powerful time-frequency signal-processing tool which allows the analysis of sampled signals with distortions. It converts waveforms into a series of wavelets which provides a way of analyzing data bounded in both frequency and duration. In recent times, such transforms are being widely used to solve power system problems requiring transient analysis.

Basically, the DWT divides the frequency-band of the input signal into low and high-frequency components, which are called here as approximation (c) and detail (d) coefficients, respectively. Such components are normally obtained by low and high-pass filters ($h(k)$ and $g(k)$, respectively) in cascade with down-samplers whose grade is of 2 .

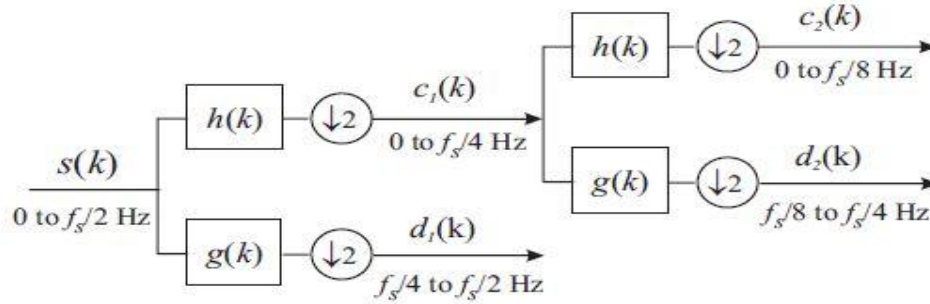


Fig. 1. DWT filter bank framework.

Fig. 1.1 illustrates the structure of a two-level DWT algorithm applied to an input signal $s(k)$ sampled at a rate of f_s Hz.

The coefficients of both $h(k)$ and $g(k)$ filters depend on the selected mother wavelet. Hence special importance is given while selecting the mother wavelet to carry out the filter analysis. In this work, the Daubechies 4 (db4) and Daubechie 6 (db6), are used which are mother wavelets quite suitable for detection of fast transients such as those induced by HIF in the transmission and distribution networks.

1.3 PROBLEM STATEMENT :

To analyze and detect High Impedance Faults (HIF) using a transients based approach i.e, Discrete Wavelet Transform(DWT) on transmission and distribution grid networks.

Using software simulations (offline) for HIF modeling and detection, extract HIF characteristics and demonstrate fast rising energies during fault inception in power system. This is achieved by performing DWT on Grid voltages and current signals at different buses from a simulated WSCC 9-Bus test case system. This groundwork is again used for hardware implementation (online) for real-time fault detection using DWT.

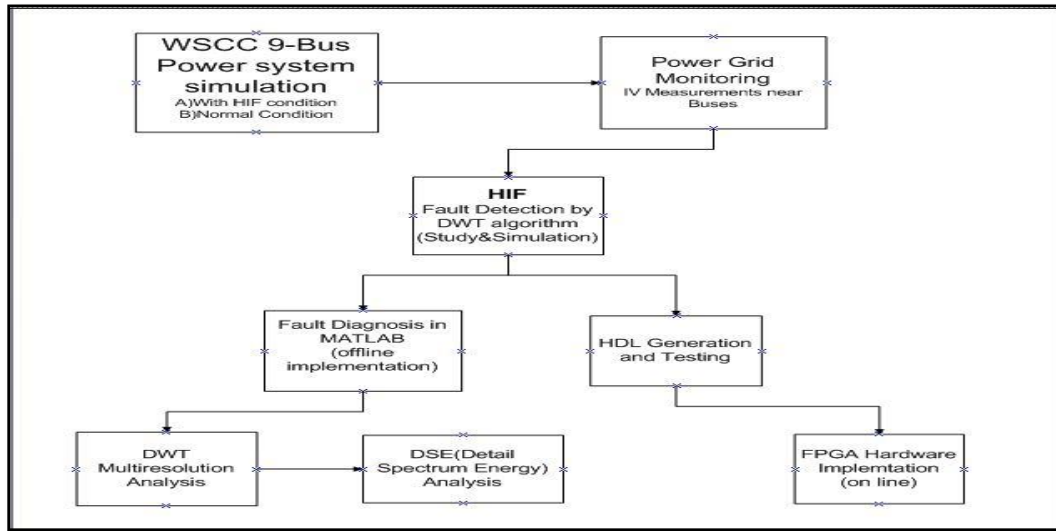


Fig 1.2 Process flow for fault detection

1.4 Organization Of Thesis

Chapter 2 discusses topics relevant to the thesis. These include fault analysis techniques using mainly the discrete wavelet transform and also briefly discussing short time fourier transform. Chapter 3 then presents a statement of the problems to be solved. These include designing in software platforms and using DWT algorithm for fault detection and identification. Chapter 4 discusses the solution methodology applied to the problems formulated. Chapter 5 then presents overall results of the wavelet detector's performance. Finally, Chapter 6 provides final conclusions and suggestions for future work.

CHAPTER 2

HIGH IMPEDANCE FAULTS (HIF) AND FAULT ANALYSIS

HIFs on electrical transmission and distribution networks involve arcing and/or nonlinear characteristics of fault impedance which cause cyclical pattern distortions. Therefore, the objective of most detection schemes is to evaluate the special features in patterns of the voltages and currents in HIFs. This chapter provides theory and formulations of the concepts that are relevant to the work carried out. First we briefly review basic fault analysis concepts and then move on to understand Wavelet Transform and the DWT technique. The Short-Time Fourier Transform offers basic concepts needed to understand discrete wavelet transform better, hence it is also discussed briefly.

2.1 Fault Analysis

Firstly it involves the determination of voltages (V) & currents (I) samples at a number of buses and lines of the power system during fault and after fault condition .

Distributed systems commonly consist of 1Φ , 2Φ and 3Φ lines, serving different types of dispersed customer loads. Faults occur when one or more phases of distributed lines come in contact with ground, another phase or object. Typically these events are due to animals, lightning, tree limbs, poor weather conditions, automobile accidents, etc. shorting or grounding one or more phases. These contingencies are unsafe to the public and often can damage conductors, insulators, or support structures and can result in extended loss of service for customers. For these reasons it is of utmost importance to detect the occurrence of all system faults, as well as determine which phase(s) are affected, as quickly as possible in order to clear the faults.

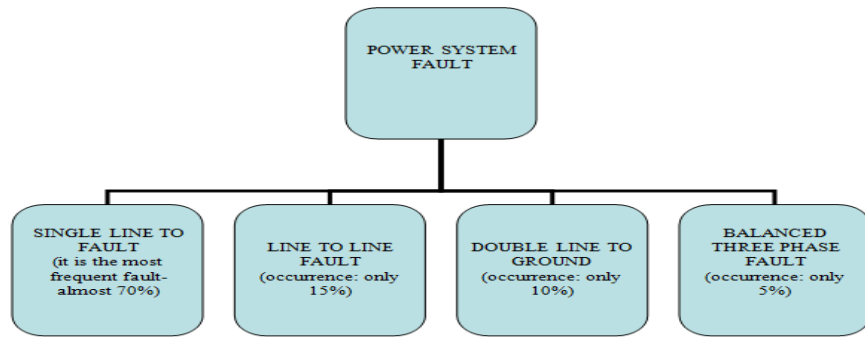


Figure2.1 Fault Classification

The line faults are typically classified as follows:

- Line-to-Ground (LG)
- Line-to-Line (LL)
- Line-to-Line-Ground (LLG)
- Three-Phase (3P)
- Three-Phase-to-Ground (3PG)

At the inception of each type of fault, voltage and current transients occur in the distribution system. The relative magnitude of the transients depends on the number of phases involved and whether the fault is grounded and even on presence of arcing.

HIF FAULT Model

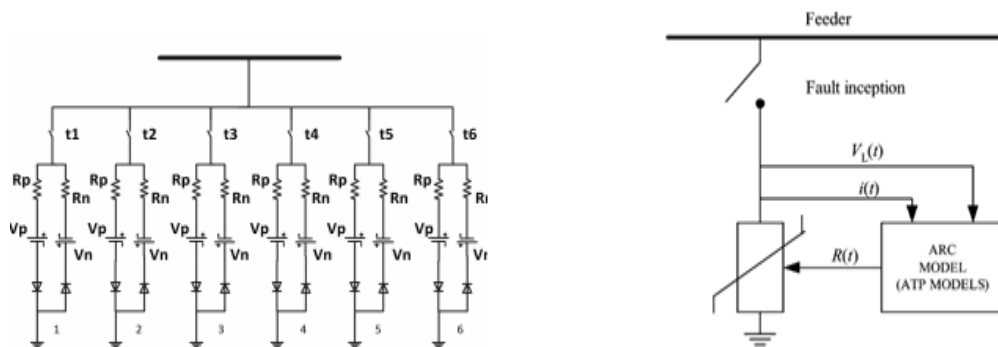


Fig2.2 Emanuel HIF Arc model (left) used to simulate High Impedance Fault(HIF) characteristics .

HIFs on electrical transmission and distribution networks involve arcing and/or nonlinear characteristics of fault impedance which cause cyclical pattern distortions. Therefore, the objective of most detection schemes is to evaluate the special features in patterns of the voltages and currents in HIFs

There can be various HIF models used for generating high impedance faults in power systems , the above figure shows HIF model used in carrying out the simulations.

Following are typical HIF induced Current and voltage characteristics:

- 1) **Asymmetry:** The fault current has different absolute values for + and - half cycle;
- 2) **Nonlinearity:** The voltage-current characteristic curve is nonlinear;
- 3) **Buildup:** The current magnitude increases gradually to its maximum value;
- 4) **Shoulder:** Buildup is ceased for few cycles.
- 5) **Intermittence:** Some cycles in which energized wire interrupts contact with soil.

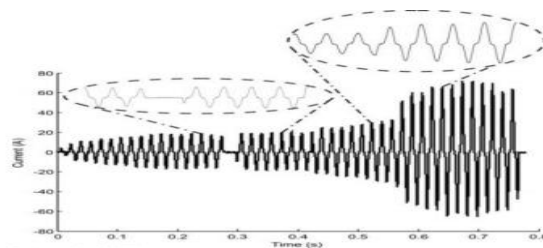


figure 2.3 Typical HIF current

Line-Line(LL) and Line-Ground (LG) Faults

Figure 2.4 below shows a circuit representation of a LL fault on phases A and B. The fault currents are indicated per phase by the notation I_{fa} , I_{fb} , and I_{fc} respectively. The fault impedance is indicated by Z_f and is dependent on certain conditions such tree limb, weather and ground conditions etc which would result in disruptions of normal feeder voltages and current supply in power system i.e fault condition.

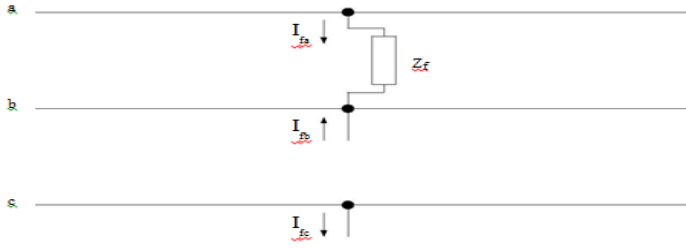


Figure 2.4 :Three-phase circuit diagram of a Phase A-to-B, LL fault. The fault current for phases a, b, and c are I_{fa} , I_{fb} , and I_{fc} respectively. Z_f is the fault impedance

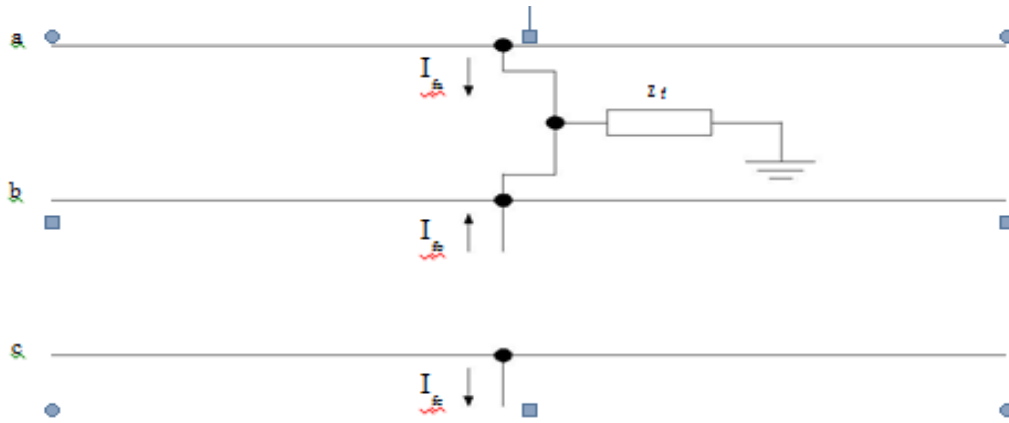


Figure 2.5:Three-phase circuit diagram of a Phase A-to-B-to-Ground, LLG fault. The fault current for phases a, b, and c are I_{fa} , I_{fb} , and I_{fc} respectively. Z_f is the fault impedance.

A larger fault current is expected for grounded faults than ungrounded faults; whereas the unaffected phases should remain similar to before inception. The fault can be due to a momentary and repetitive High impedance or a momentary or persistent low impedance path in the power distribution and transmission networks. If it's a the common ground or phase faults, then the circuit breakers and protection equipment detect that a contingency has occurred and allow them to open the respective phases. But we will focus on detecting the HIF faults which are not easily detectable by traditional protection systems.

2.2 Wavelet Transform:

The wavelet transform (WT) is the newer mathematical tool which can be used for signal processing with a wide variety of applications, e.g. transient analysis, acoustics, communications, etc. The main reason for this growing activity is the ability of the wavelet not only to decompose a signal into its frequency components but provide information in time domain as well. It provides a non-uniform division of the frequency domain, whereby it allows the decomposition of a signal into different levels of resolution. The basis function (mother wavelet) is dilated at low frequencies and compressed at high frequencies, so that large windows are used to obtain the low frequency components of the signal, while small windows are used for High frequency component .

This attribute to tailor the frequency resolution can greatly facilitate signal analysis and detection of signal features, which can be very useful in characterizing the source of the transients and /or the state of the post-disturbance system. The WT normally uses both the analysis and synthesis wavelet pair. Synthesis is used when the waveform is to be reconstructed.

In wavelet analysis, the original signal is decomposed into its constituent wavelet sub-bands or levels. Each of these levels represents that part of the original signal occurring at that particular time and in that particular frequency band. These individual frequency bands are logarithmically spaced rather than uniformly spaced as in Fourier analysis. This makes the decomposed signals possess a powerful time-frequency localization property, which is one of the major benefits provided by WT. The resulting decomposed signals

can then be analyzed in both time and frequency domains

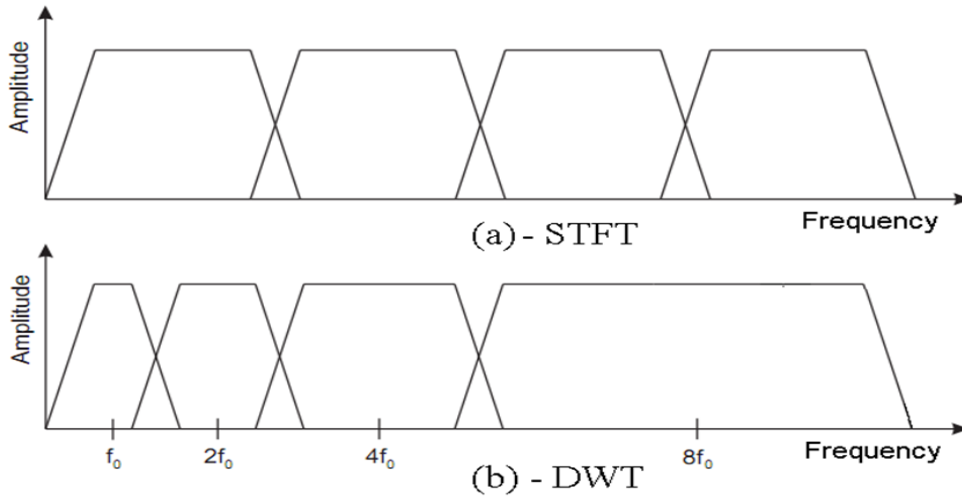


Figure 2.6 Showing STFT DWT windows.

2.3 Fault Detection Using the Discrete Short Time Fourier Transform (DSTFT)

The Discrete Fourier Transform (DFT) has been widely used in the past and even now to analyze the frequency spectrum of periodic, stationary signals. This allows for localization in frequency but very poor localization in time. When applied to non-stationary signals the DFT is therefore able to identify the frequencies that are present in a particular signal, but has difficulty determining when they had occurred. In order to improve time-frequency localization the Discrete Short-Time Fourier Transform (STFT) was developed. The STFT differs from the DFT by multiplying the original signal by a Hamming window, essentially a band-pass filter, of fixed length and translating it over the length of the sampled signal (0.1).

$$X_n(e^{j\omega_k m}) = \sum x(m) w(n-m) e^{-j\omega_k m} \quad (0.1)$$

where:

$x(m)$: the signal to be analyzed,

$w(m)$: the window function of fixed length L

$\omega_k = 2\pi k/N$: the frequency in radians with N frequency bands

As long as $L \leq N$ perfect reconstruction is possible. The size of the window function is directly related to the frequency range allowed to pass through the filter. A smaller window therefore has better frequency resolution by allowing high frequencies to pass through it; conversely, a larger window will have better resolution in time by allowing lower frequencies to pass through. If several frequency ranges are of interest, the STFT must be run with each of the corresponding window sizes.

2. 4 Discrete Wavelet Transform (DWT) and Multi-Resolution Analysis (MRA)

The wavelet transform is a mathematical tool that divides up data, functions or operators into different frequency components and then studies each component with a resolution matched to its scale. Basically, wavelet transforms are divided into two, namely:

Continuous Wavelet Transform (CWT) and Discrete Wavelet Transform

(DWT). Since most operations are now performed using computers, which use digital forms of data, the latter is preferred by most researchers and is used in this study.

The DWT analyses the original signal at different frequency bands with different resolutions by decomposing the signal into a coarse approximation and detail information

In doing this, the DWT employs two sets of functions called *Scaling functions* ($\phi_{j,k}$) and

Wavelet functions ($\psi_{j,k}$). These are respectively associated with high and low pass

filters.

The objective of multi-resolution analysis (MRA) is to develop representation of a sophisticated signal, $f(t)$ in terms of wavelet and scaling functions . It is designed to produce good time resolution and poor frequency resolution at high frequencies and good frequency resolution and poor time resolution (larger periods) at low frequencies. The idea behind this is that most signals encountered in practical applications have high frequency components for short durations and low frequency components for long durations.

The scaling (a) coefficients, otherwise known as approximation , are a low-resolution representation of the original signal, i.e. it is the high-scale, low frequency components of a signal. It is computed by taking the inner products of the function $f(t)$ with the scaling basis $\varphi_{j,k}$ as illustrated in eqn (0.2)

$$A_{j,k} = \left\langle f(t), \varphi_{j,k} \right\rangle = \int_{-\infty}^{\infty} f(t), \varphi_{j,k}(t) dt \quad (0.2)$$

The wavelet (d) coefficients, otherwise known as detail , represent high frequency components of the original signal. In the application of the DWT in waveform realization ,different WT coefficients are attained at different decomposition scales. Scale 1 (d1) is the shortest mother wavelet and contains the highest frequency information present in the input signal; scale 2 (d2) the next highest, and so on . This is evident and can be computed by taking the inner products of the function, $f(t)$ with the wavelet basis $\psi_{j,k}$ as presented in eqn (0.3).

$$D_{j,k} = \left\langle f(t), \psi_{j,k} \right\rangle = \int_{-\infty}^{\infty} f(t), \psi_{j,k}(t) dt \quad (0.3)$$

where j is the resolution level and k , the length of the filter vector.

The scale function $\varphi_{j,k}(t)$ and wavelet function $\psi_{j,k}(t)$ are determined by the selection

of a particular mother wavelet $\psi(t)$ like db4 ,db 6 or haar which have their set of scaling and wavelet basis functions which are shifted and translated as in eqns (0.4) and (0.5) respectively

$$\begin{aligned}\varphi_{j,k}(t) &= 2^{j/2} \varphi(2^j t - k) \\ \psi_{j,k}(t) &= 2^{j/2} \psi(2^j t - k)\end{aligned}\quad (0.4),(0.5)$$

The effect of the decomposition scales is illustrated later in simulation results for three ,five and nine different scales of db4 on an input signal. The details and approximations of the original signal $f(t)$ are obtained by passing it through a filter bank, which consists of low and high pass filters. The low pass filter removes the high frequency components, while the high-pass filter picks out the high-frequency contents in the signal being analyzed. The low-pass and the high-pass filters are determined by the scaling function and the wavelet function, respectively. The maximum number of wavelet decomposition levels for WT is determined by the length of the original signal, the particular wavelet being selected, and also, the level of detail required.

2.4.1 DWT Filter Banks (HPF & LPF) and Multi Resolution Analysis MRA :

The wavelet transform offers an alternative approach to using the STFT for the analysis of **short-time, high frequency transients**. The transform is performed similarly to the STFT, except that the “windowing function” is variable in size. This windowing function, also known as a Mother Wavelet, must possess several criteria in order to be admissible. These include oscillatory or wave-like behavior (pulses), an average value of zero about the time axis (x-axis) and quick decay to zero . The Mother Wavelet is then subject to a scaling/dilation function and is translated across the desired signal. Like the Fourier transform, the wavelet transform also has a parallel in discrete time called DWT.

$$f[n] = \frac{1}{\sqrt{M}} \sum_k W_\phi[j_0, k] \phi_{j_0, k}[n] + \frac{1}{\sqrt{M}} \sum_{j=j_0}^{\infty} \sum_k W_\psi[j, k] \psi_{j, k}[n]. \quad (0.6)$$

$$W_\phi[j_0, k] = \frac{1}{\sqrt{M}} \sum_n f[n] \phi_{j_0, k}[n].$$

$$W_\psi[j, k] = \frac{1}{\sqrt{M}} \sum_n f[n] \psi_{j, k}[n] \quad j \geq j_0. \quad (0.7) \text{ \& } (0.8)$$

Each dilation and translation of the Mother Wavelet is called a Daughter Wavelet, and produces an associated wavelet coefficient, whose sum allows for signal reconstruction. Larger scaling values correspond to larger window sizes, yielding better time resolution and utility in the analysis of low frequencies. Conversely, smaller scaling values correspond to smaller window sizes, yielding better frequency resolution and utility in the analysis of high frequencies. The resulting wavelet coefficients for each scale show how well the signal and wavelet match. This leads to an important property of the wavelet transform, Multi-Resolution Analysis (MRA).

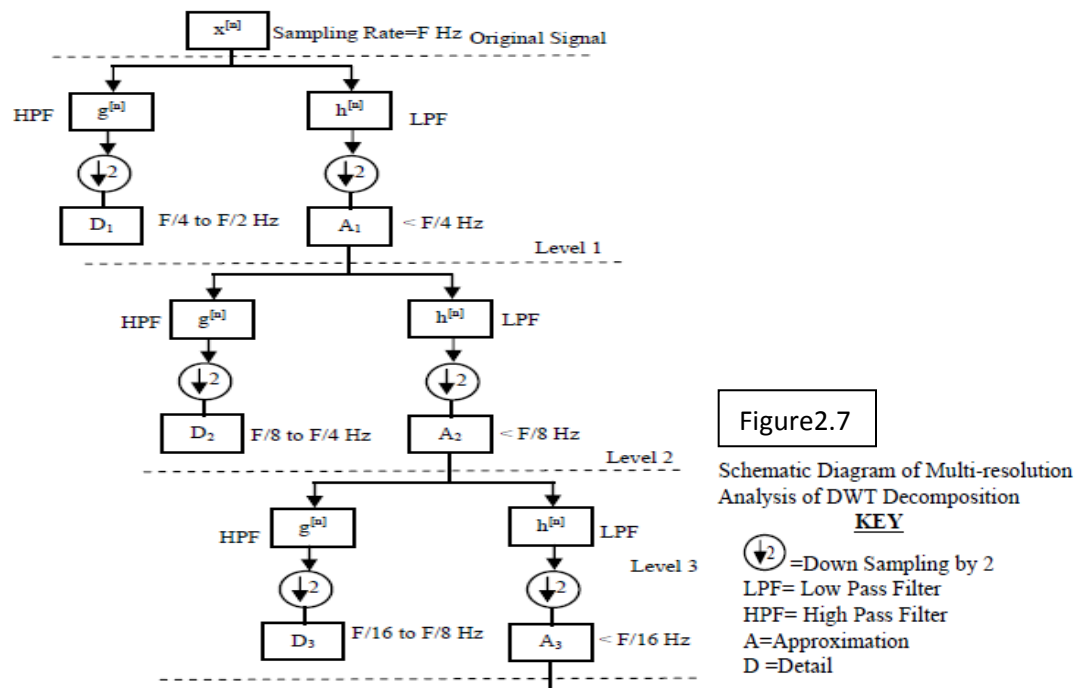
The above equation can be compared to a Finite Impulse Response (FIR) filter used often in signal processing. It can therefore be constructed using a filter bank consisting of high- and low-pass filters whose outputs are odd-indexed, alternating reversed-versions of each other. These are more commonly termed quadrature mirror filters.

Brief Review:

At each level the signal is passed through a high- and low pass filter. The output of the high pass filter is directly related to the higher frequency components of the original signal.

The resulting “detail” coefficients represent the signal detail at a frequency related to the

scale of the mother wavelet. Similarly the output of the low pass filter results in a smoother, less detailed version of the signal directly related to the lower frequency components. This output is then down-sampled by a factor of 2 and used as the input for the next level of high- and low-pass filters. The detail coefficients from successive high-pass filters represent increasing signal detail, which is directly related to higher frequency components of the original signal. The output of successive low pass filters continues to smoothen the original signal for use at the next level of filters. This procedure is possible, so long as sampled data remains to continue down sampling. Graphical representation is shown below.



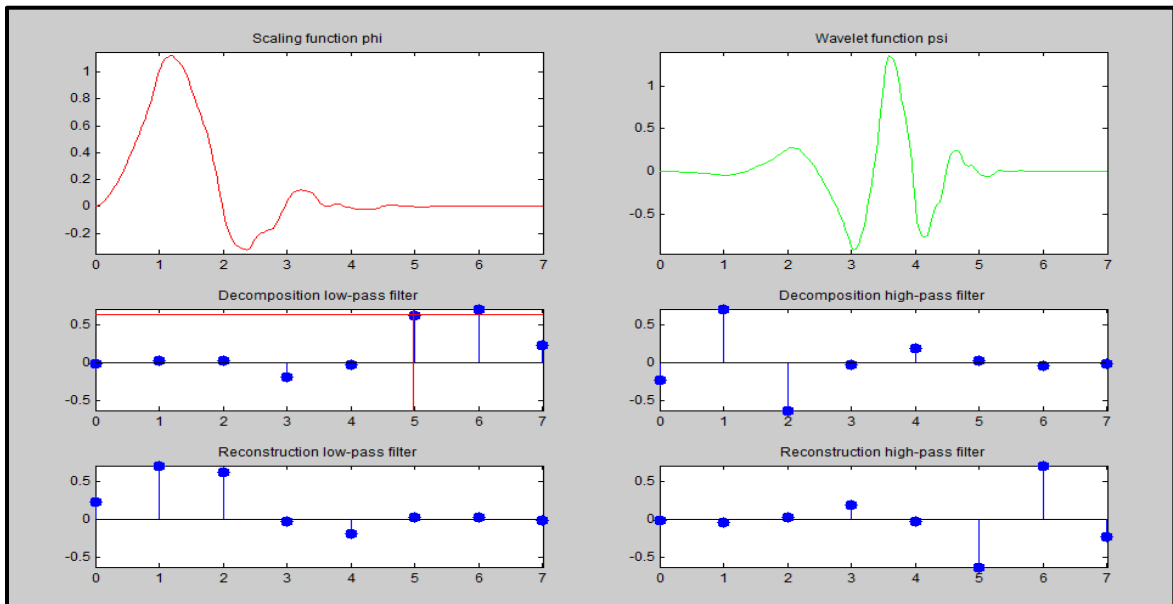
Down-sampling by a factor of 2 greatly reduces redundancy by effectively discarding half of the samples at each level with minimal to no loss of accuracy. This provides a computational advantage over the STFT and perfect or near perfect reconstruction is still possible by reversing the decomposition process and up-sampling by a factor of 2 at each level.

2.4.2 DWT Filter Coefficients (HPF-g(k) & LPF-h(k)) and Scaling, Wavelet functions :

Db4 Wavelet Filter coefficients

1. $h_0 = -0.0105974018$	1. $g_0 = -0.2303778133$
2. $h_1 = 0.0328830117$	2. $g_1 = 0.7148465706$
3. $h_2 = 0.0308413818$	3. $g_2 = -0.6308807679$
4. $h_3 = -0.1870348117$	4. $g_3 = -0.0279837694$
5. $h_4 = -0.0279837694$	5. $g_4 = 0.1870348117$
6. $h_5 = 0.6308807679$	6. $g_5 = 0.0308413818$
7. $h_6 = 0.7148465706$	7. $g_6 = -0.0328830117$
8. $h_7 = 0.2303778133$	8. $g_7 = -0.0105974018$

Figure 2.8 Scaling, Wavelet functions and Filter coefficients for DB4 Wavelet



Db6 Wavelet Filter coefficients:

1. $h_0 = -0.0010773011$	$g_0 = -0.1115407434$
2. $h_1 = 0.0047772575$	$g_1 = 0.4946238904$
3. $h_2 = 0.0005538422$	$g_2 = -0.7511339080$
4. $h_3 = -0.0315820393$	$g_3 = 0.3152503517$
5. $h_4 = 0.0275228655$	$g_4 = 0.2262646940$
6. $h_5 = 0.0975016056$	$g_5 = -0.1297668676$
7. $h_6 = -0.1297668676$	$g_6 = -0.0975016056$
8. $h_7 = -0.2262646940$	$g_7 = 0.0275228655$
9. $h_8 = 0.3152503517$	$g_8 = 0.0315820393$
10. $h_9 = 0.7511339080$	$g_9 = 0.0005538422$
11. $h_{10} = 0.4946238904$	$g_{10} = -0.0047772575$
12. $h_{11} = 0.1115407434$	$g_{11} = -0.0010773011$

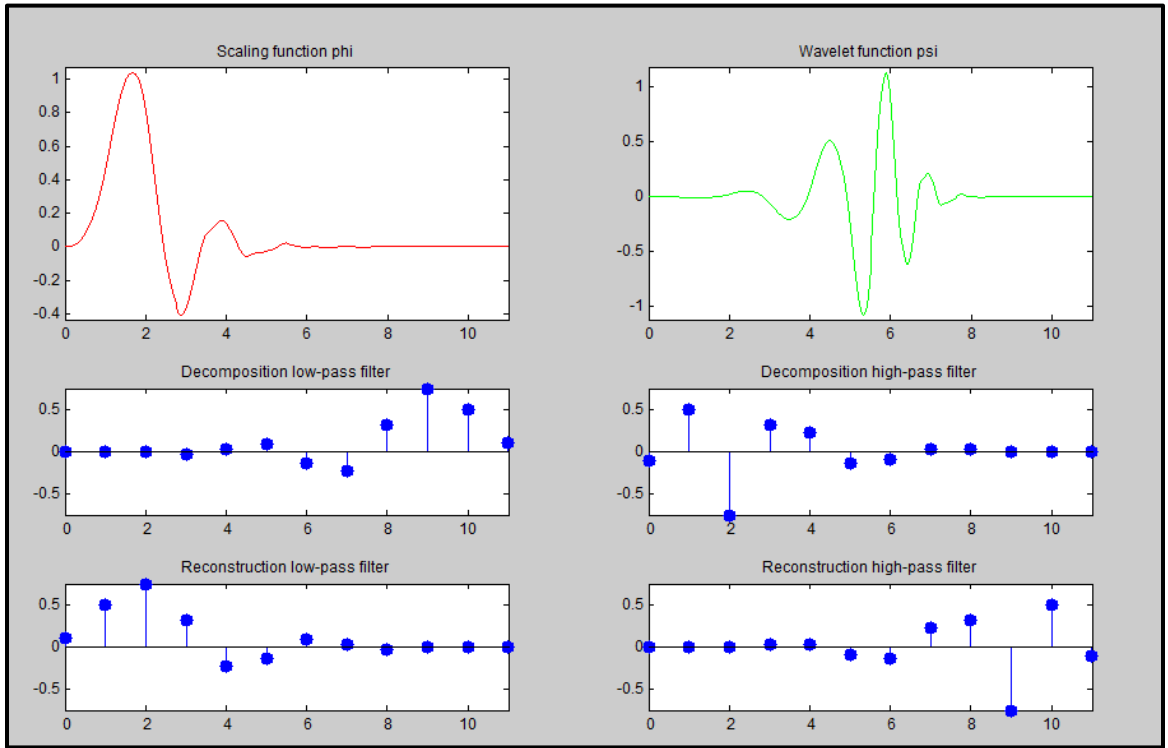


Figure 2.9 Scaling, Wavelet functions and Filter coefficients for DB6 Wavelet

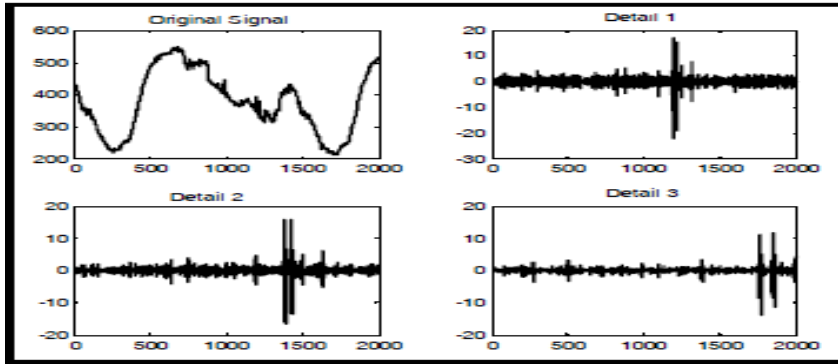


Figure 2.10 Different Decomposition Scales of Daubechies Wavelet of a random signal

2.5. Energy Spectrum of Detail Coefficients

Several fault diagnosis techniques use the detail coefficients to detect monitored signal high frequency transient components which arise due to faults along with the normal signals. However, electrical noises may pose a difficult for such methods, since they can be mistakenly confused with fault-induced transients. This problem becomes more evident for the HIF case, where voltage and current induced transients are commonly

attenuated.

To overcome the electrical noise problem, the energy spectrum of detail coefficients ‘d’ — here referred as ξ_j — is used. According to the computation of the energy at a scale j may be successfully performed using a moving data window that goes through d samples, shifting one coefficient at a time such as follows:

$$\xi_j(k) = \sum_{n=k}^{k + \frac{\Delta k_{cycle}}{2^j}} d_j^2(n) , \quad (0.9)$$

Δk_{cycle} the number of samples in one power frequency cycle of the input signal.

Aiming the reduction of the algorithm computational burden, only detail coefficients at the first scale (j = 1) are analyzed, i.e., is computed using only detail coefficients d1 for fast computations.

Energy of voltage ξ_v and energy of current ξ_i

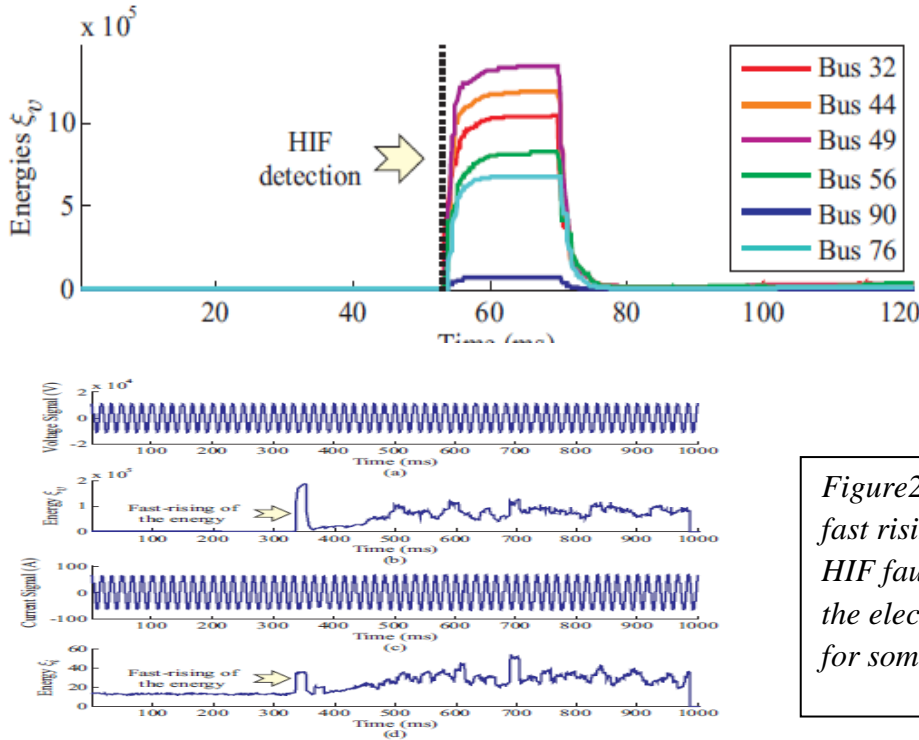


Figure 2.11 and 2.12 showing fast rising transients indicating HIF fault at different points in the electrical power network for some test system.

One can see that the HIF beginning time is unclear in both presented voltage and current records, whereas the fast-risings in energies v and i permit the detection of the moment in which fault-induced transients begin at the monitored terminal. Hence, the proposed algorithm is implemented here in such way that both voltage and current waveform samples are generally used for getting the high frequency detail coefficients.

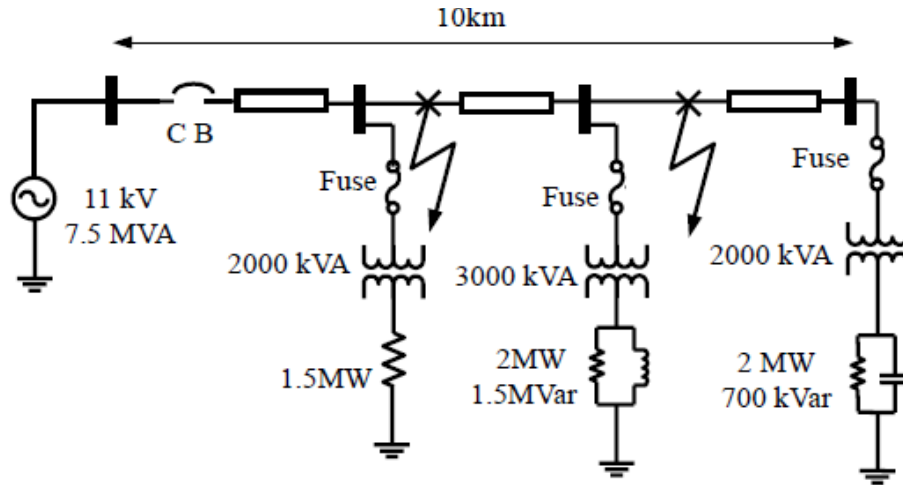


Fig 2.13 One-line diagram of an example radial distribution feeder.

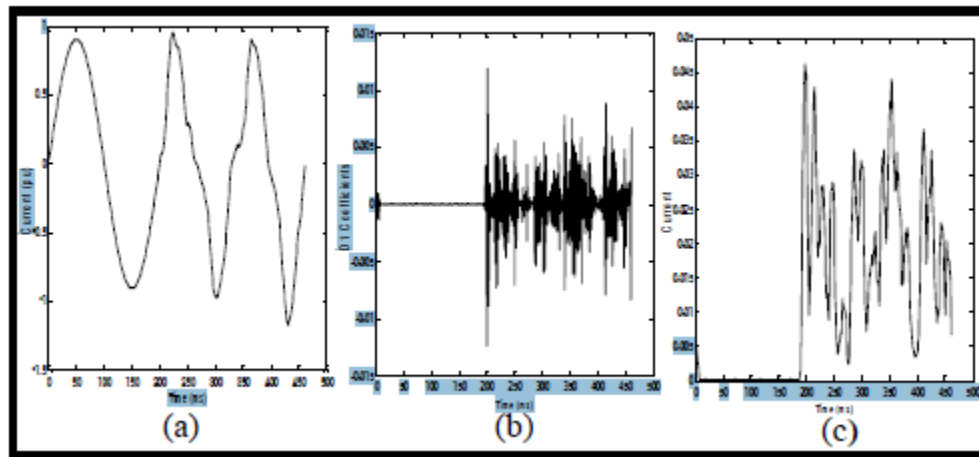


Figure 2.14 HIF Current Waveform, D1 Coefficients and its Detection

CHAPTER 3

PROBLEM FORMULATION AND SOLUTION METHODOLOGY

3.1 FORMULATION:

Objective:

To analyze and detect High Impedance Faults (HIF) in electrical grid network with a transients based approach DWT algorithm . Use software simulations (offline) for HIF Fault modeling in electrical network and carry out fault detection and HIF feature extractions by DWT algorithm. Demonstrate fast rising of energies in power system, which indicate fault inception times, with detail energy spectrum (DSE) obtained from (Discrete Wavelet Transform) DWT of Grid voltages and currents for a simulated WSCC 9-Bus test case system. This groundwork is again used for hardware implementation (online) for real-time fault detection using DWT by setting appropriate thresholds for fault detection and HIF identification.

The high impedance fault arc impedance can be modeled through resources as shown below.

High Impedance Fault (HIF) Model

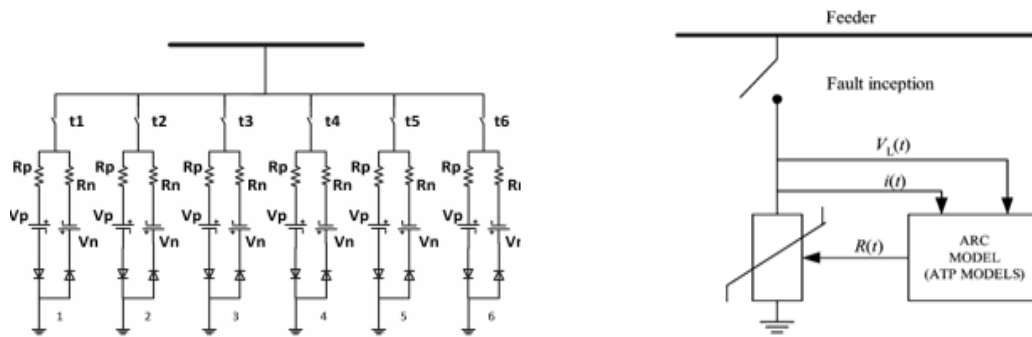


Figure 3.1 HIF Emanuel model (left) and time varying non-linear resistor(right) model

$$D_{j,k} = \langle f(t), \psi_{j,k} \rangle = \int_{-\infty}^{\infty} f(t), \psi_{j,k}(t) dt$$

$$A_{j,k} = \langle f(t), \varphi_{j,k} \rangle = \int_{-\infty}^{\infty} f(t), \varphi_{j,k}(t) dt$$

For Multi Resolution Analysis:

$$\varphi_{j,k}(t) = 2^{j/2} \varphi(2^j t - k)$$

$$\psi_{j,k}(t) = 2^{j/2} \psi(2^j t - k)$$

DSE CALCULATION:

$$\xi_j(k) = \sum_{n=k}^{k + \frac{\Delta k_{cycle}}{2^j}} d_j^2(n) ,$$

3.2 SOLUTION METHODOLOGY:

For applications to power system problems, a fault detection and identification algorithm for a 230kV EHV transmission line was studied. The system consisted of a generator at the sending end, which is connected to a load at the receiving end through long transmission lines. The Daubechies-4&6 wavelets were chosen due to its computation speed and accuracy for both high and low frequency events. Sampling frequency was chosen to be 40Khz for voltage and current signals. The algorithm checks the 1,2,3,4,5 and 6 level detail coefficient for current and voltage samples that and then evaluates the detail energies for currents and voltage for 5khz -15khz frequency ranges .The fast rising detail energies signify that a High impedance fault has occurred and also helps eliminate noise factor for better results. This also provide better information about threshold setting and threshold violations to detect and classify HIF and other faults. The maximum absolute values of these coefficients compared for all three phases. This determines which phases are affected by the fault. This process is then repeated for higher(7th 8th

9th..) level coefficients in order to extract more detail or information with regard to the lower frequency bands or the fundamental frequency.

. The resulting detail values and their pattern (regular or irregular distortion cycles) at appropriate resolution levels can be compared to four other threshold values , which classify the fault as HIF, LLL, LG, LL or an LLG fault. More stress has to be placed on setting the thresholds as there are problems distinguishing between LL,LG,LLG faults due to an overlap in the range of the detail coefficient magnitudes .Overall the algorithm performed very well at detecting HIF faults.

CHAPTER 4

A CASE STUDY: WSCC9-BUS 3-GENERATOR SYSTEM

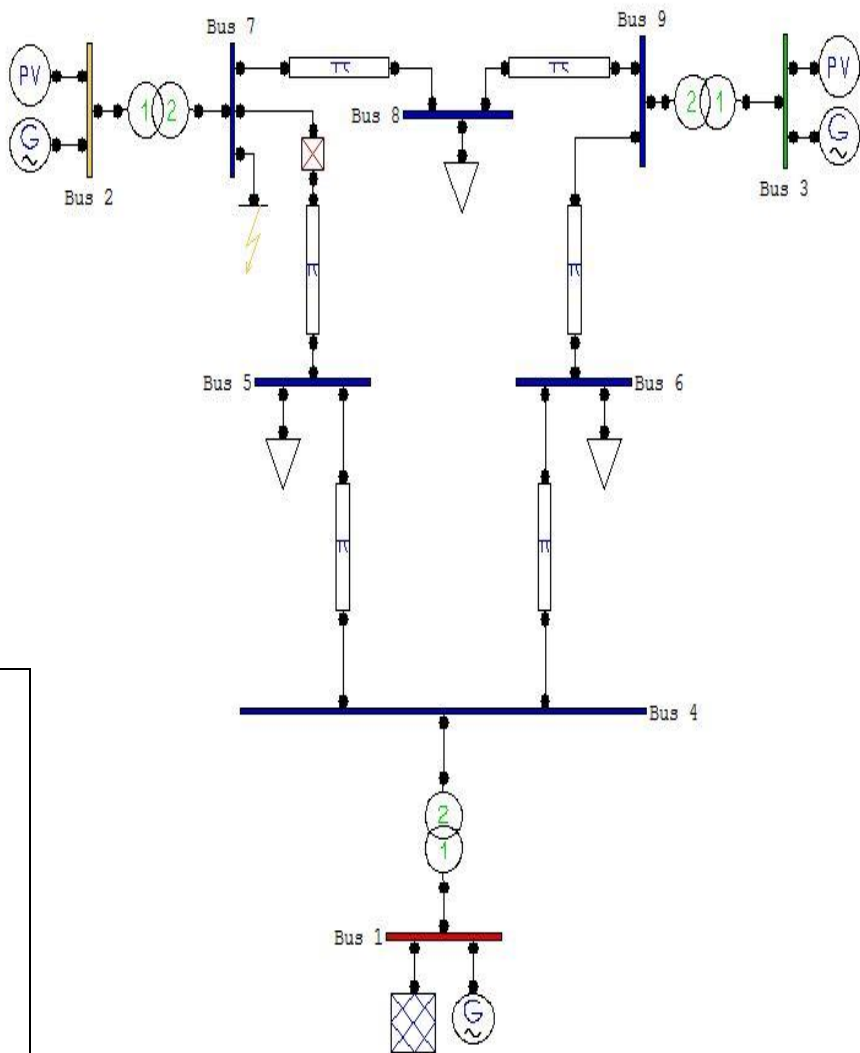
Basically, this 9 bus system contains 3 generators, 9 buses and 3 loads.

The base KV levels in the go from 16.5 kV to 230 kV. The line complex powers are around hundreds of MVA each. As a test case, this one has few voltage control devices and is easy to control.

NETWORK STATISTICS	
Buses:	9
Lines:	6
Transformers:	3
Generators:	3
Loads:	3

GENERATOR ,BUS DATA	
Bus1 (slack)	16.5KV 243MVA
Bus 2 (PV)	192MVA 18KV
Bus 3 (PV)	128MVA 13.8KV
Bus 5 (PQ)	125MW 50MVAR
Bus 6 (PQ)	90MW 30MVAR
Bus 8 (PQ)	100MW 35MVAR
Generators:	3
Loads:	3

GLOBAL SUMMARY REPORT	
TOTAL GENERATION	
REAL POWER [p.u.]	3.1964
REACTIVE POWER [p.u.]	0.2284
TOTAL LOAD	
REAL POWER [p.u.]	3.15
REACTIVE POWER [p.u.]	1.15
TOTAL LOSSES	
REAL POWER [p.u.]	0.04641
REACTIVE POWER [p.u.]	-0.9216



4.1 WSCC 9-BUS 3-GENERATOR single line diagram in PSAT

POWER FLOW DATA:

Powergui Load Flow Tool, model: IEEE_9bus_new_o															
	Block type	Bus type	Bus ID	Vbase (kV)	Vref (pu)	Vangle (deg)	P (MW)	Q (Mvar)	Qmin (Mvar)	Qmax (Mvar)	V_LF (pu)	Vangle_LF (deg)	P_LF (MW)	Q_LF (Mvar)	Block Name
1	Vsrc	swing	BUS_1	16.50	1.0400	0.00	0.00	0.00	-Inf	Inf	0.00	0.00	0.00	0.00	247.5 MVA, 16.5 kV
2	Bus	-	BUS_4	230.00	1	0.00	0.00	0.00	0.00	0.00	0.00	0.00	0.00	0.00	Load Flow Bus1
3	RLC load	PQ	BUS_5	230.00	1	0.00	125.00	50.00	-Inf	Inf	0.00	0.00	0.00	0.00	125 MW 50 MVAR/Three-Phase Par...
4	RLC load	PQ	BUS_6	230.00	1	0.00	90.00	30.00	-Inf	Inf	0.00	0.00	0.00	0.00	90 MW 30 MVAR/Three-Phase Para...
5	Bus	-	BUS_7	230.00	1	0.00	0.00	0.00	0.00	0.00	0.00	0.00	0.00	0.00	Load Flow Bus4
6	Bus	-	BUS_9	230.00	1	0.00	0.00	0.00	0.00	0.00	0.00	0.00	0.00	0.00	Load Flow Bus5
7	RLC load	PQ	BUS_8	230.00	1	0.00	90.00	30.00	-Inf	Inf	0.00	0.00	0.00	0.00	100 MW 35 MVAR/Three-Phase Par...
8	Vsrc	PV	BUS_2	18.00	1.0250	0.00	163.00	0.00	-Inf	Inf	0.00	0.00	0.00	0.00	192 MVA, 18 kV
9	Vsrc	PV	BUS_3	13.80	1.0250	0.00	85.00	0.00	-Inf	Inf	0.00	0.00	0.00	0.00	128 MVA, 13.8 kV

Bus	V	phase	P gen	Q gen	P load	Q load
	[p.u.]	[rad]	[p.u.]	[p.u.]	p.u.]	[p.u.]
Bus 1	1.04	0	0.71641	0.27046	0	0
Bus 2	1.025	0.16197	1.63	0.06654	0	0
Bus 3	1.025	0.08142	0.85	-0.1086	0	0
Bus 4	1.0258	-0.03869	0	0	0	0
Bus 5	0.99563	-0.06962	0	0	1.25	0.5
Bus 6	1.0127	-0.06436	0	0	0.9	0.3
Bus 7	1.0258	0.06492	0	0	0	0
Bus 8	1.0159	0.0127	0	0	1	0.35
Bus 9	1.0324	0.03433	0	0	0	0

LINE FLOW DATA

LINE FLOWS						
From Bus	To Bus	Line	P Flow	Q Flow	P Loss	Q Loss
			[p.u.]	[p.u.]	[p.u.]	[p.u.]
Bus 9	Bus 8	1	0.24183	0.0312	0.00088	-0.21176
Bus 7	Bus 8	2	0.7638	-0.00797	0.00475	-0.11502
Bus 9	Bus 6	3	0.60817	-0.18075	0.01354	-0.31531
Bus 7	Bus 5	4	0.8662	-0.08381	0.023	-0.19694
Bus 5	Bus 4	5	-0.4068	-0.38687	0.00258	-0.15794
Bus 6	Bus 4	6	-0.30537	-0.16543	0.00166	-0.15513
Bus 2	Bus 7	7	1.63	0.06654	0	0.15832
Bus 3	Bus 9	8	0.85	-0.1086	0	0.04096
Bus 1	Bus 4	9	0.71641	0.27046	0	0.03123

LINE FLOWS						
From Bus	To Bus	Line	P Flow	Q Flow	P Loss	Q Loss
			[p.u.]	[p.u.]	[p.u.]	[p.u.]
Bus 8	Bus 9	1	-0.24095	-0.24296	0.00088	-0.21176
Bus 8	Bus 7	2	-0.75905	-0.10704	0.00475	-0.11502
Bus 6	Bus 9	3	-0.59463	-0.13457	0.01354	-0.31531
Bus 5	Bus 7	4	-0.8432	-0.11313	0.023	-0.19694
Bus 4	Bus 5	5	0.40937	0.22893	0.00258	-0.15794
Bus 4	Bus 6	6	0.30704	0.0103	0.00166	-0.15513
Bus 7	Bus 2	7	-1.63	0.09178	0	0.15832
Bus 9	Bus 3	8	-0.85	0.14955	0	0.04096
Bus 4	Bus 1	9	-0.71641	-0.23923	0	0.03123

Different types of HIF Faults being simulated at BUS-7, I-V signals taken at BUS7,BUS5 &BUS4 for phases A,B&C.

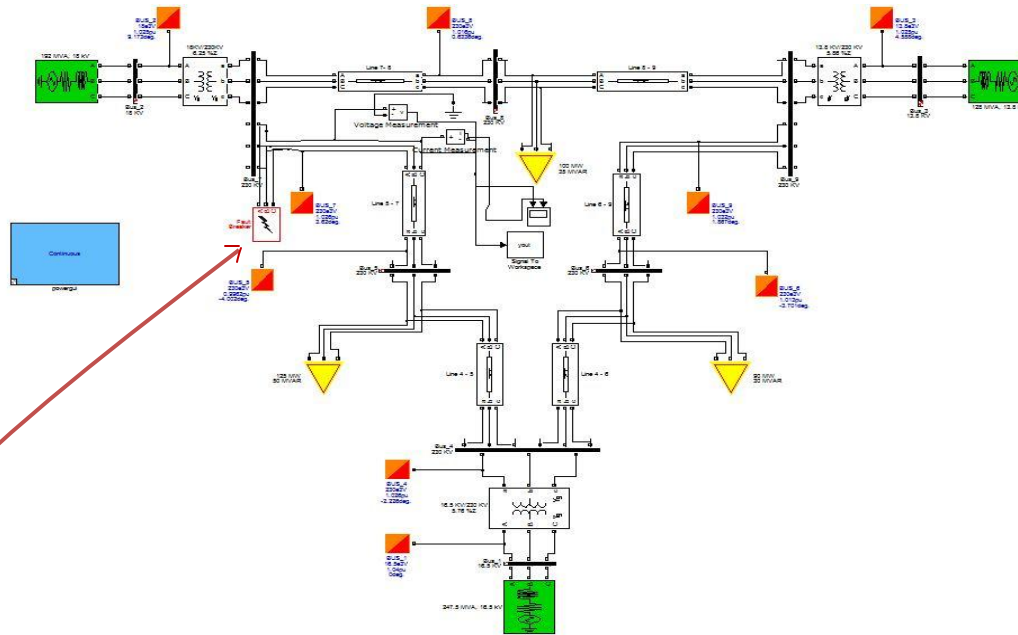
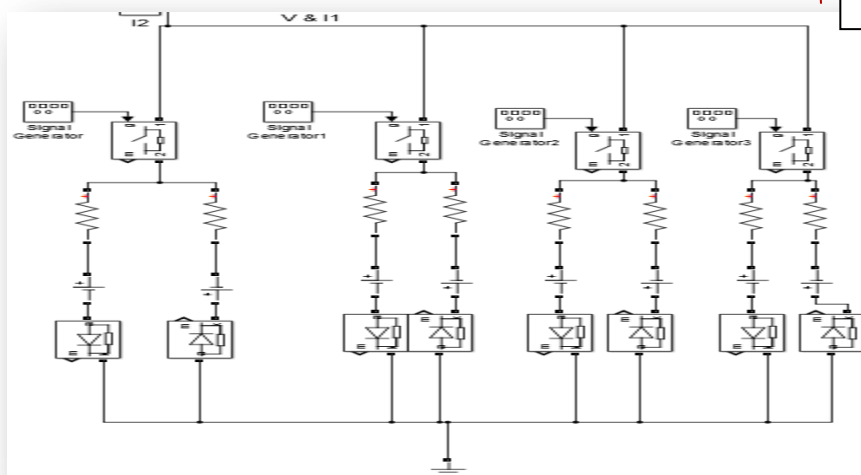


Figure:4.2 WSCC(Western State Coordinating Council) 9-BUS 3-GENERATOR Test system in SIMULINK Different types of Faults including HIF being simulated at BUS-7, I-V signals taken at BUS7,BUS5&BUS4 for phases A,B &C.



HIF Emanuel model applied at Bus 7

Voltage profiles at different buses

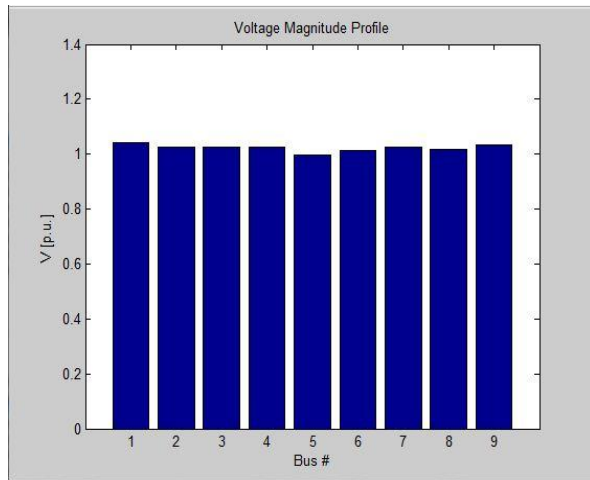


Figure 4.3

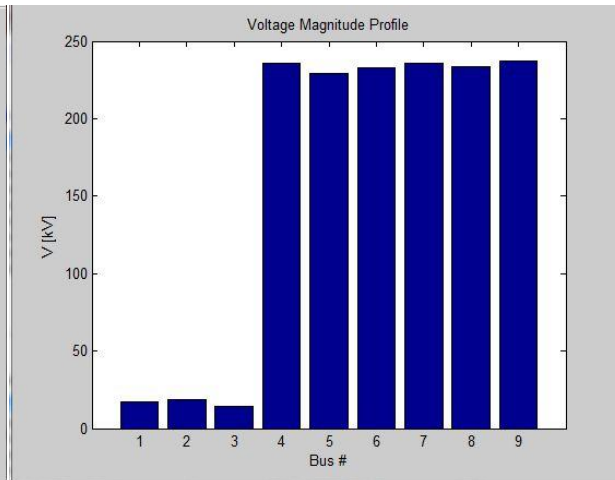


Figure 4.4,

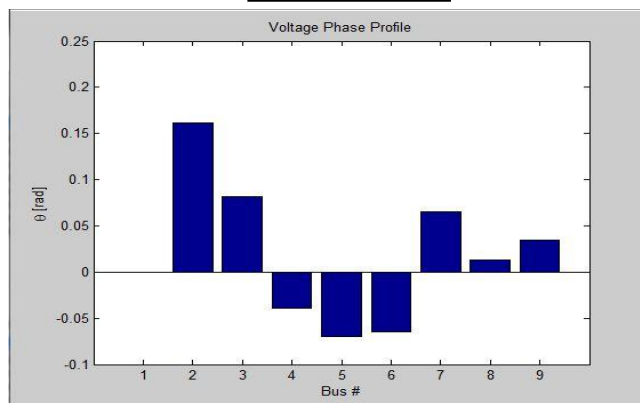


Figure 4.5,

Power profiles at different buses

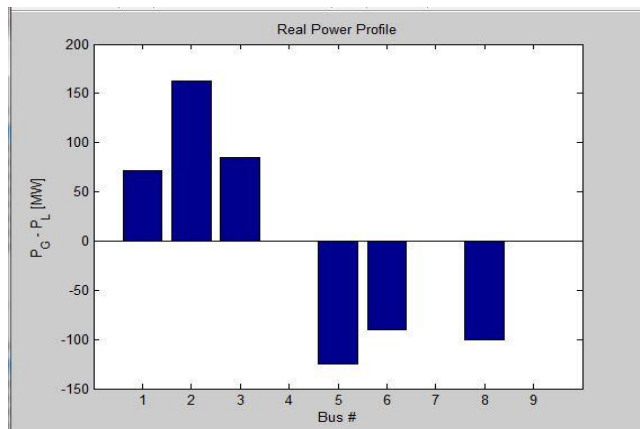


Figure 4.6

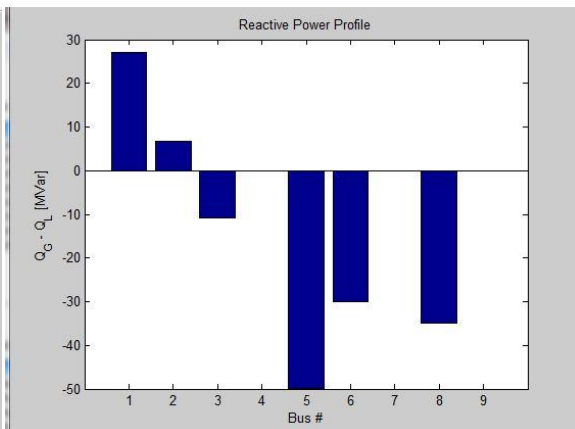


Figure 4.7

Chapter5 Simulation Results

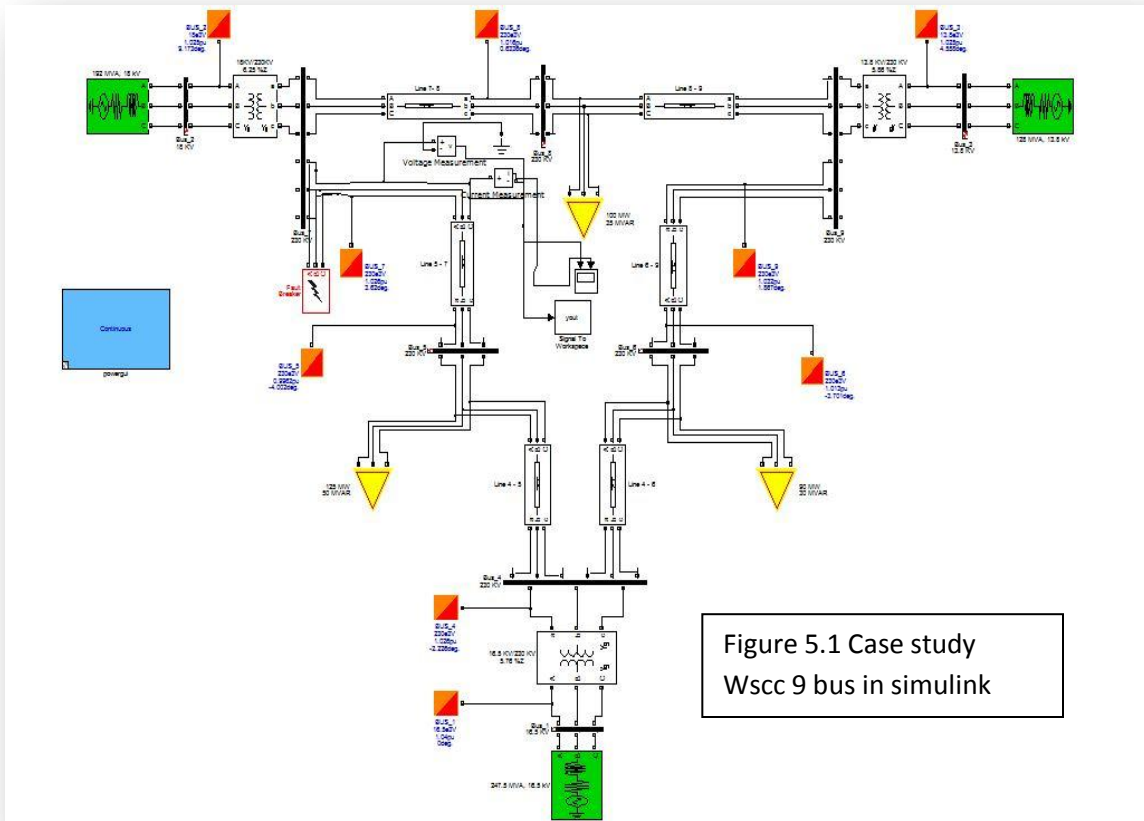
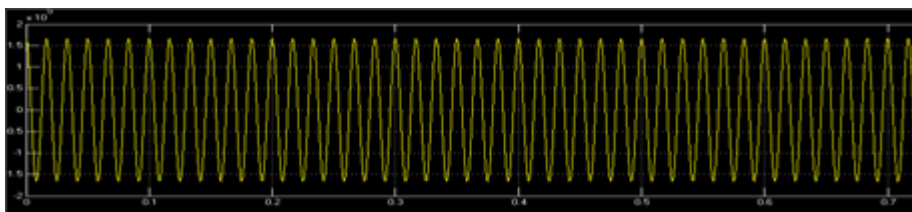
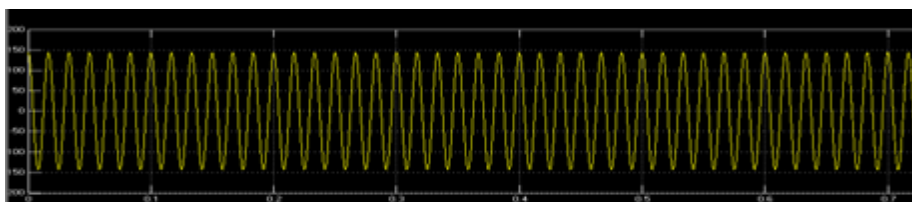


Figure 5.1 Case study
Wsc9 bus in simulink

5.1 Normal (No fault) condition simulation:



(a) Voltage



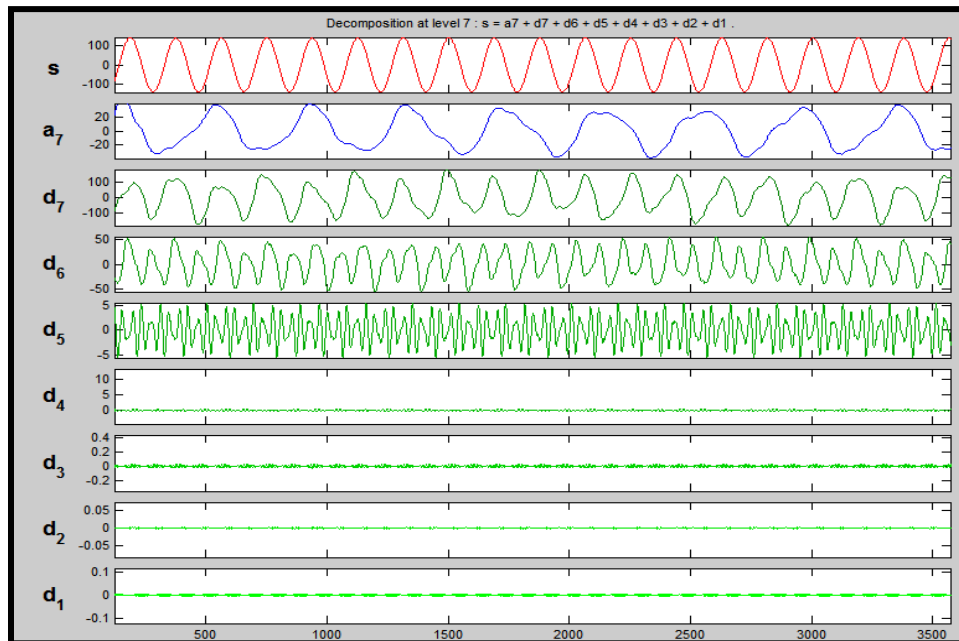
(a) Current

Monitoring V-I at WSCC BUS7 phase C

(a) V_7 voltage(top)

(b) I_7 current (bottom)

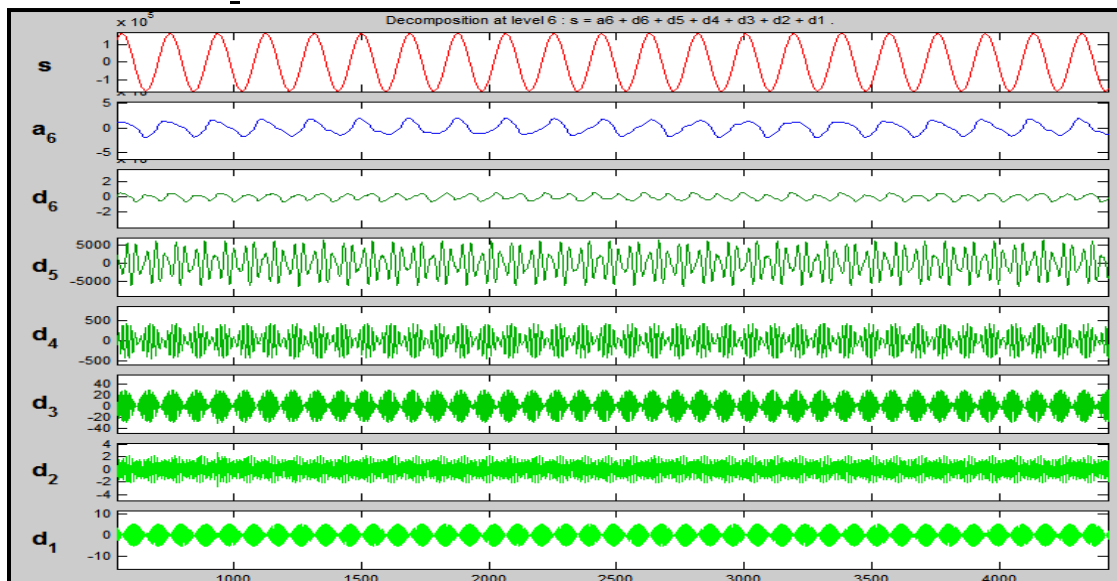
Analyzing Ic_7: Bus7 (Phase C)current signal using DWT algorithm (DB4 –LEVEL 6)



A Picture of detail and approximate coefficients. With **db4** wavelet (**Level 4 Resolution**)

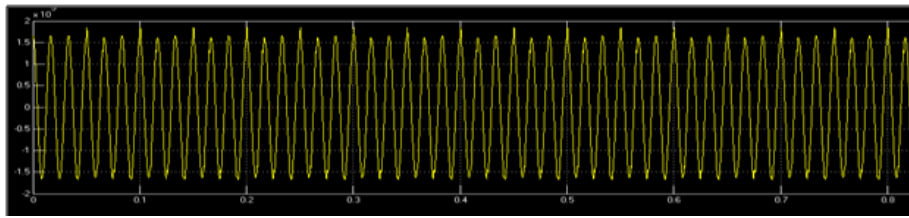
Looking at detail coefficients between d_1 to d_4 for High frequency transients i, we find no transient behavior occurring in these frequency ranges of 5khz-15 khz for normal no fault condition of operation of the WSCC 9-Bus 3-Generator System.

Analyzing Vc_7: Bus7 (Phase C)VOLTAGE signal using DWT algorithm (DB4 –LEVEL 6)

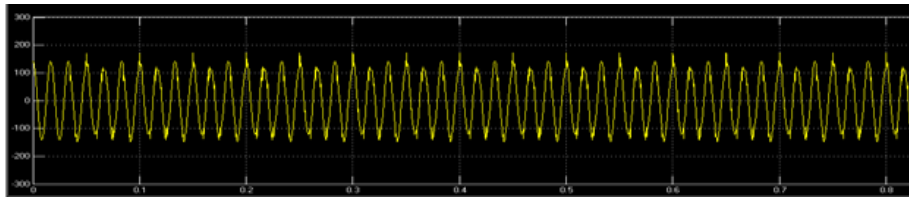


A Picture of detail and approximate coefficients. With **db4** wavelet (**Level 4 Resolution**)

5.2 High Impedance fault (HIF) simulation: (**EMANUEL HIF MODEL**)



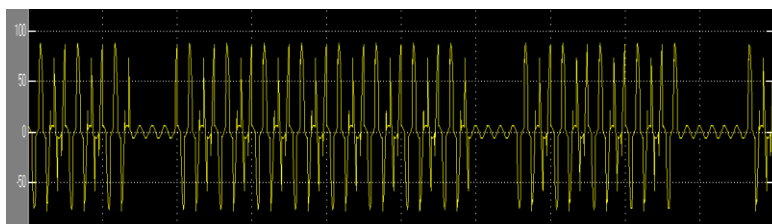
(a) Voltage V_7 at BUS 7 (order $10^5 v$)



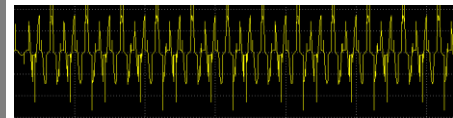
(b) Current I_7 at BUS 7(Amp)

Non- Linear Voltage –Current characteristics of fault **current (b)** and **voltage(a)** across simulated HIF model near **BUS 7(phase C)**

Transients hard to see and detect by normal protective relays.

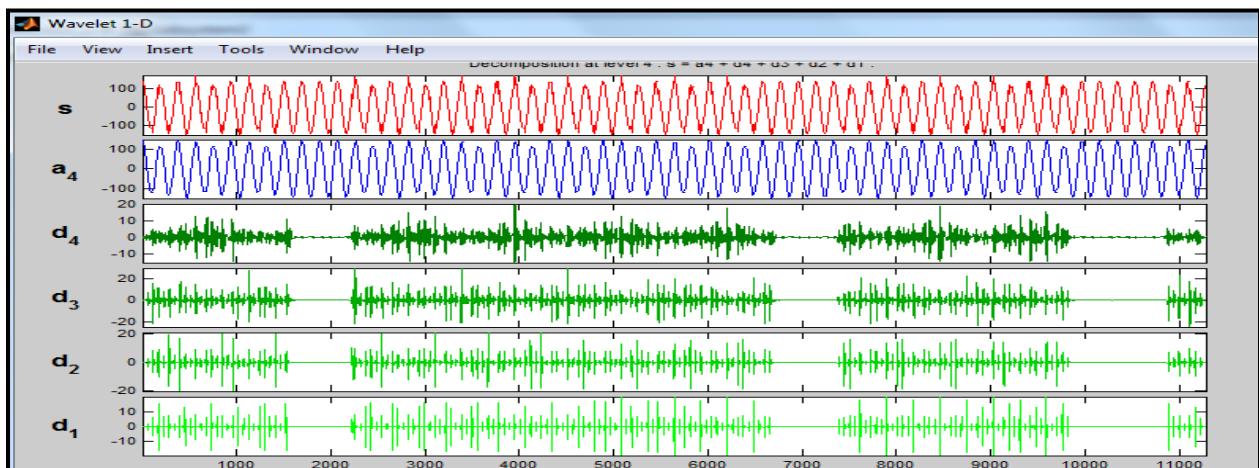


(a) Simulated Hif current through Emanuel Model .



(b) Hif current

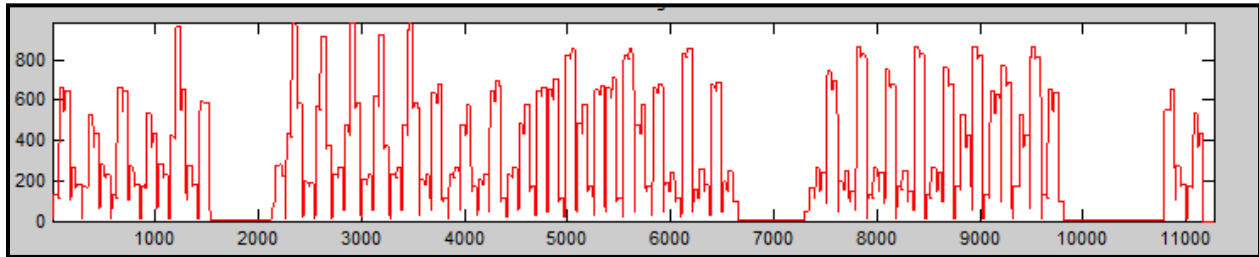
Analyzing **I_{c_7}** . Bus7 (Phase C) current signal using DWT algorithm (DB4 –LEVEL 4)



A Picture of detail and approximate coefficients. With **db4** wavelet (**Level 4 Resolution**)

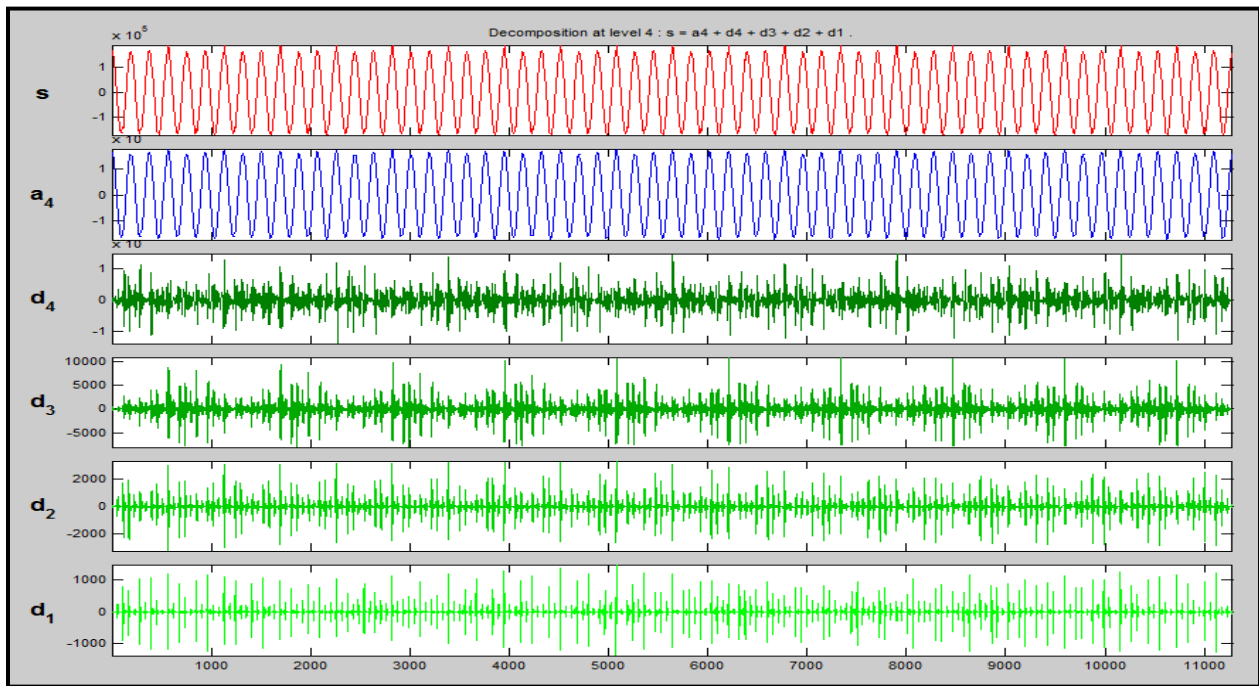
Detail Spectrum Energy (DSE) Analysis

(fast rising energies indicating fault)(\dot{E}_i for I_{c_7})



The HIF detection algorithm used here is based on the identification of fast-rising energies into _ waveforms. As depicted in Fig. above, such energies are almost constant during the steady-state and increase very fast at the disturbance inception..In some situations, as in the case of the presence of noises in voltage/current measurements, oscillations in _ may show up even during the steady-state. Hence, in order to properly detect HIF-induced transients, the hard thresholding procedure is applied here, in which energies smaller than a given threshold are discarded whereas high energy transients are detected, the average energy of this frequency band can also be used for threshold violation checks and detect HIF.

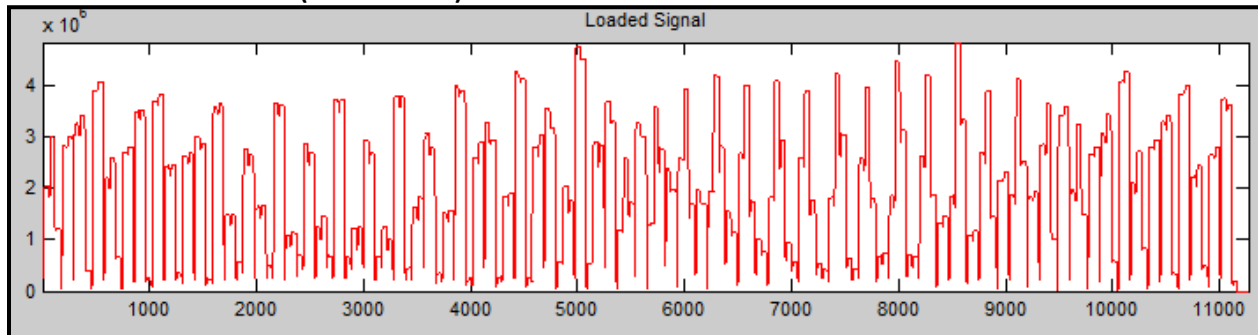
Analyzing V_{c_7} : Bus7 (Phase C) current signal using DWT algorithm (DB4 –LEVEL 4)



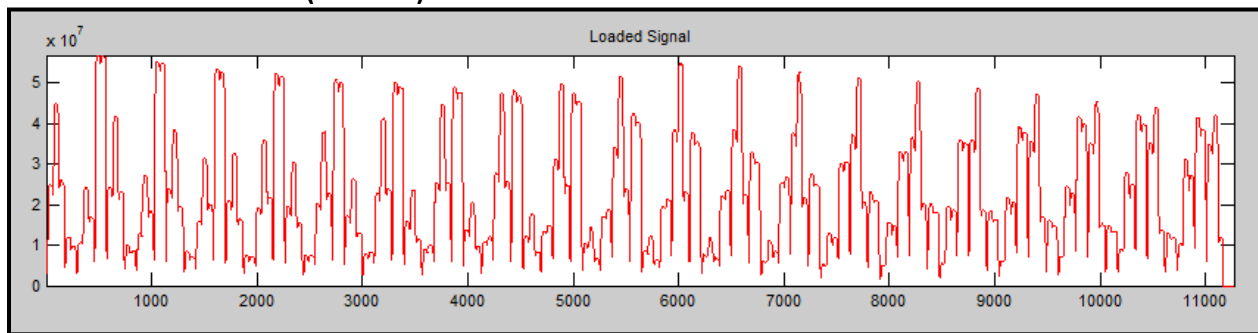
*A Picture of detail and approximate coefficients. With **db4** wavelet (Level 4 Resolution)*

Detail Spectrum Energy (DSE) Analysis (fast rising energies indicating fault)(\dot{E}_v for Vc_7)

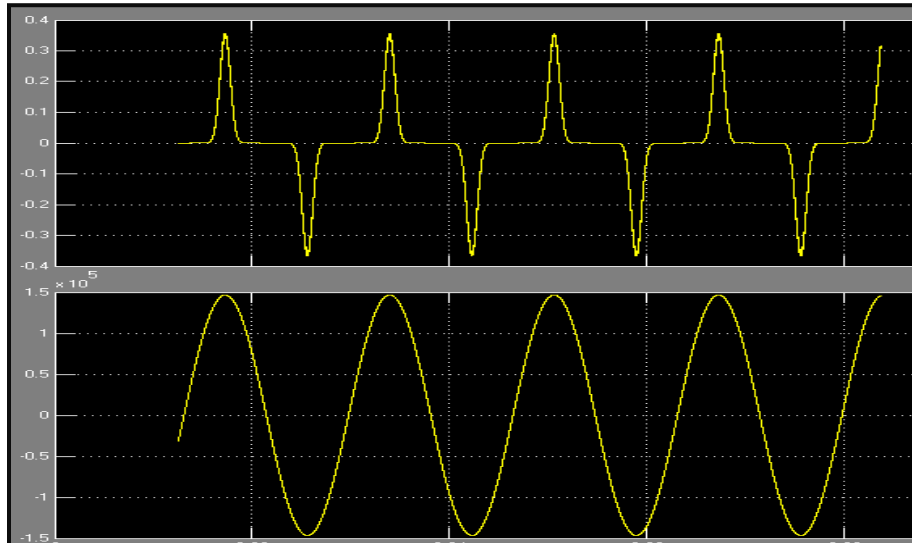
For detail 1 coefficients : (10khz-20khz)



For detail 2 coefficients: (5-10 khz)



5.2 High Impedance fault (HIF) simulation: (*time varying resistor HIF MODEL*)

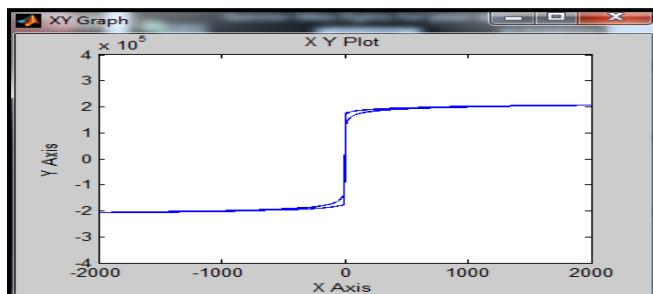


HIF at WSCC BUS7 phase C

(a) HIF current (top)

(b) Voltage across HIF model (bottom)

Non-linear time varying resistance used to simulate HIF at BUS7 phase C ..



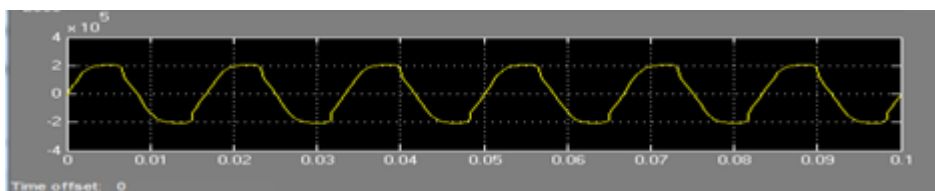
Model non-linear characteristics under 230 kv AC source.

(a) Y axis-HIF current (top);

(b) X axis-HIF Voltage (bottom)

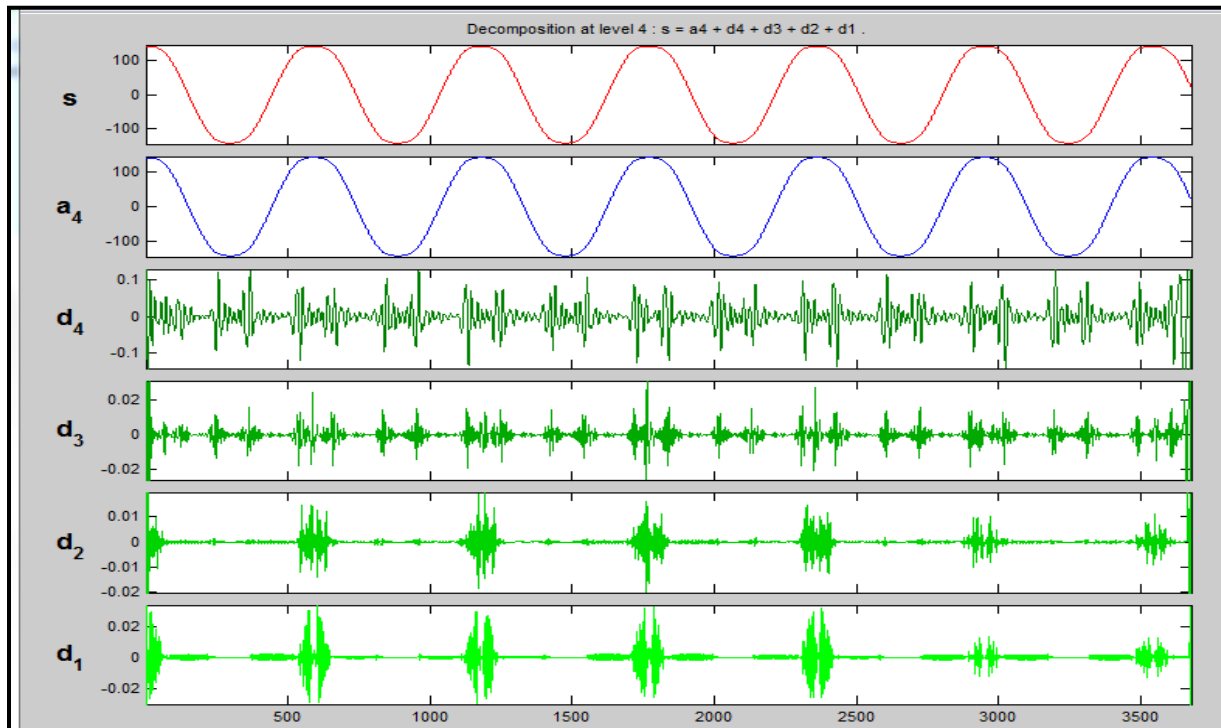


(a) Simulated Hif current through time-varying resistor model .



(b) voltage across time- varying resistor HIF Model .

Analyzing Ic_7: Bus7 (Phase C)current signal using DWT algorithm (DB4 –LEVEL 4)



*A Picture of detail and approximate coefficients. With **db4** wavelet (Level 4 Resolution)*

Transients hard to see and detect by normal protective relays.

The above figures demonstrate the results of Discrete Wavelet Transform (DWT) algorithm applied on the current samples of Bus 7 phase C feeder after inception of HIF fault which was simulated by non-linear resistor HIF fault model near BUS 7 .

The simulation was carried out for 1s and sampling was carried out at sampling frequency of 40Khz. Applying DWT on the above signal we get transients information in different frequency sub-

bands with respect to time. Following transient frequencies are contained in different detail bands.

Typical HIF induced transients lie between (2 KHz to 15KHz).

d1-(9 khz to 18khz) d2-(4.5 khz to 9 khz) d3-(2.25 khz to 4.5khz) d4(1.125 khz to 2.25 khz)

d5-(562hz to 1125 hz) d6-(282 hz to 562hz) d7-(141hz to 282hz) d8-(70hz to 141 hz)

d9 -(35hz to 70hz)---fundamental frequency 60hz signal contained a9-(0 to 35 hz)

5.3 LINE TO GROUND (L-G) FAULTS (Low Impedance Path)

- Fault inception at BUS 7 for **0.1s** duration at **t=0.83s**
- Fault Impedance **Zf=100 ohm**

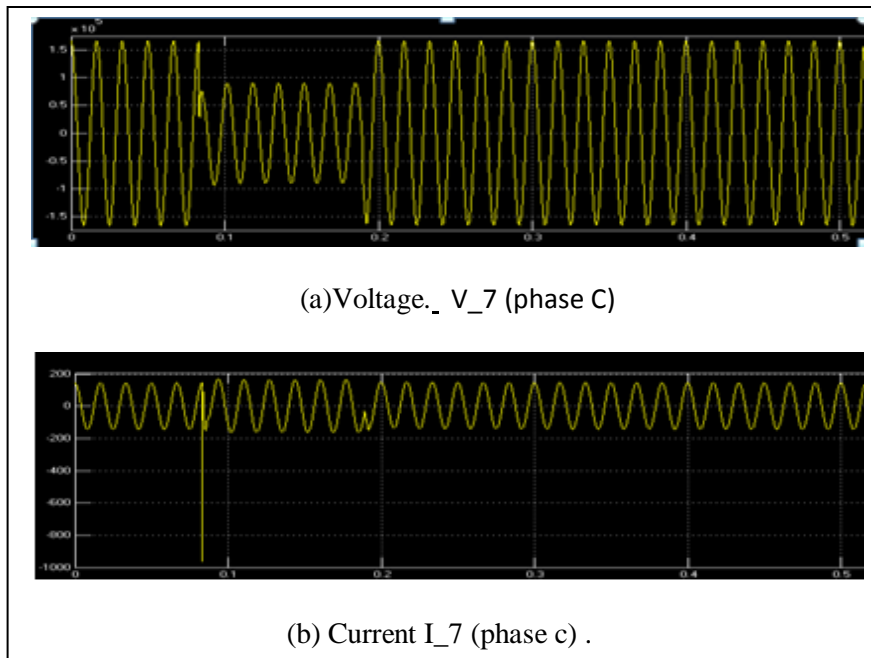


Figure 5.2 I-V AT BUS_7

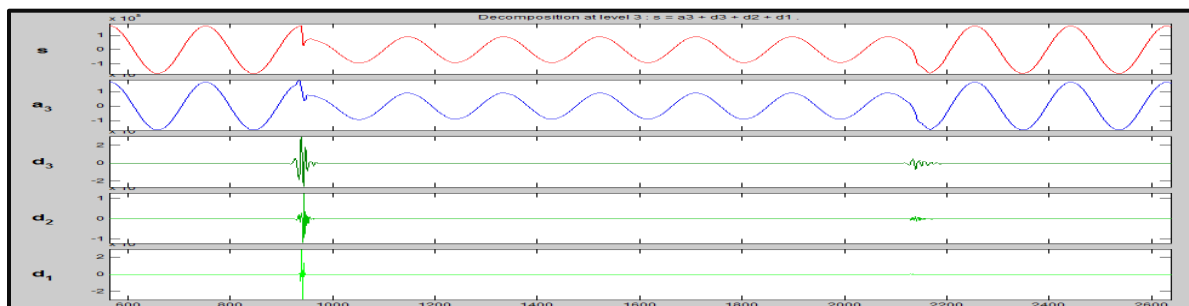
- (a) BUS 7 phase 'c' Voltage(top)
(b) BUS7 phase 'c' Current
(bottom)

Voltage(V) & Current (I) MEASUREMENT at Bus 7 for Phase C after applying (L-G) fault .

Unlike HIF case we can clearly see sudden increase in current which is generally sets the circuit breaker.

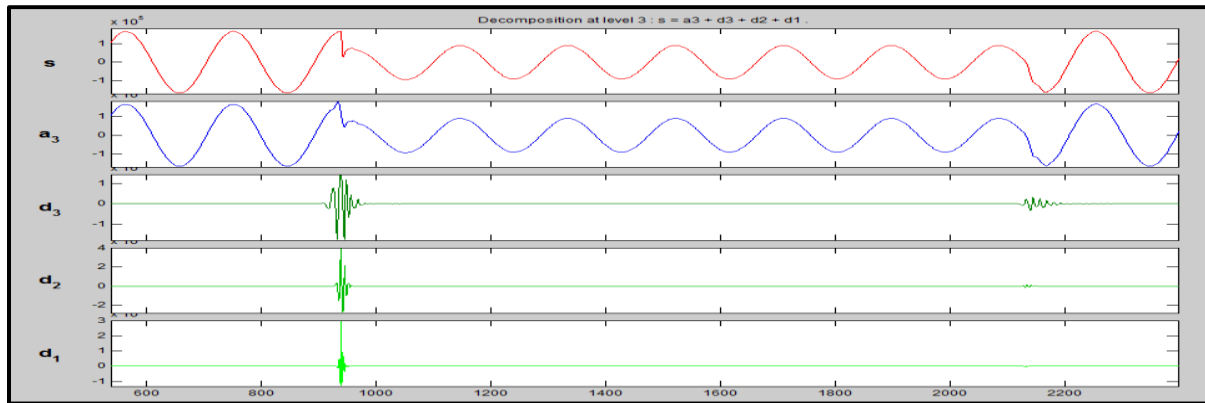
Analyzing V_c 7:Bus7 (Phase C)voltage signal using DWT algorithm

WITH db4 wavelet



A Picture of detail and approximate coefficients. With **db4** wavelet (Level 3 Resolution)

WITH db6 wavelet



*A Picture of detail and approximate coefficients. With **db6** wavelet (Level 3 Resolution)*

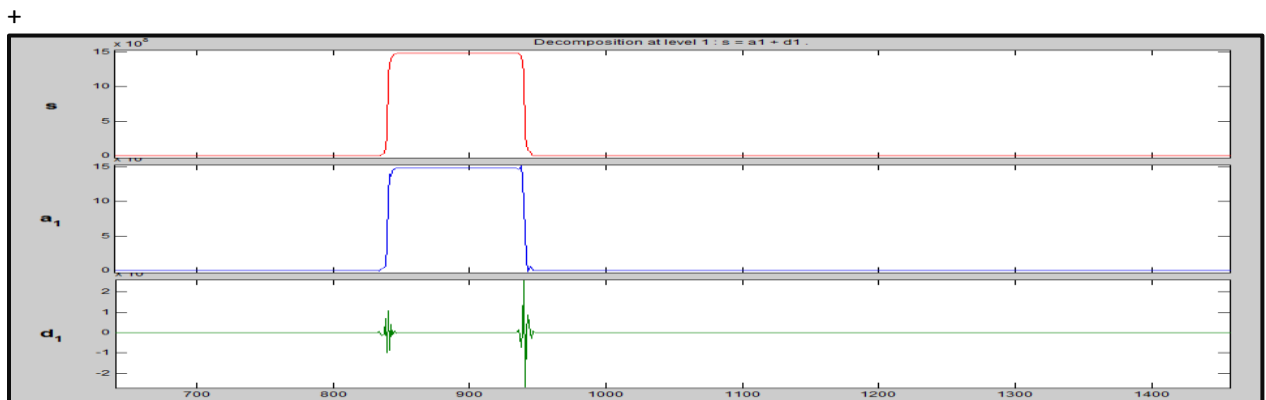
Looking at detail coefficients between d1 to d4 for High frequency transients i, we do not find significant transient behavior occurring during and post fault inception in these frequency ranges of 5khz-15 khz for L-G faults in WSCC 9-Bus 3-Generator System.

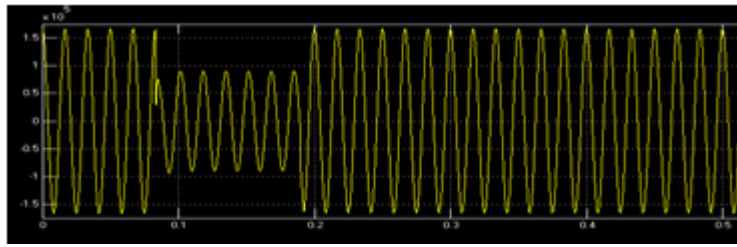
Detail coefficients tabulated

D1	-1.71332	24.74838	-11.7995	-5.94882	6.525433	-1.72557	-1.34164	2.26038	-0.12865
D2	104.023	53.80227	-64.0197	-50.976	10.80094	15.45958	17.92913	6.845963	-16.661
D3	-603.731	-388.878	5.726983	257.0155	376.4664	304.8635	97.95367	-12.7719	-79.9217

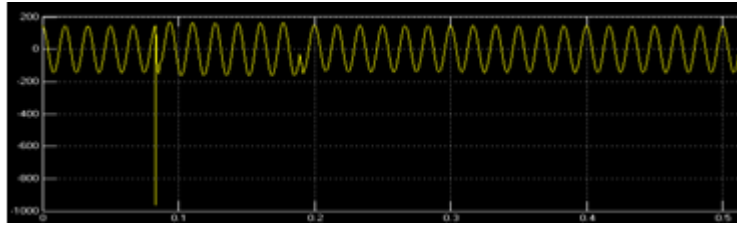
Detail Spectrum Energy (DSE) Analysis

(fast rising energies indicating fault)($\dot{\mathbf{E}}_v$ for V_{c_7})





(a) Voltage_ V_7 (phase C)



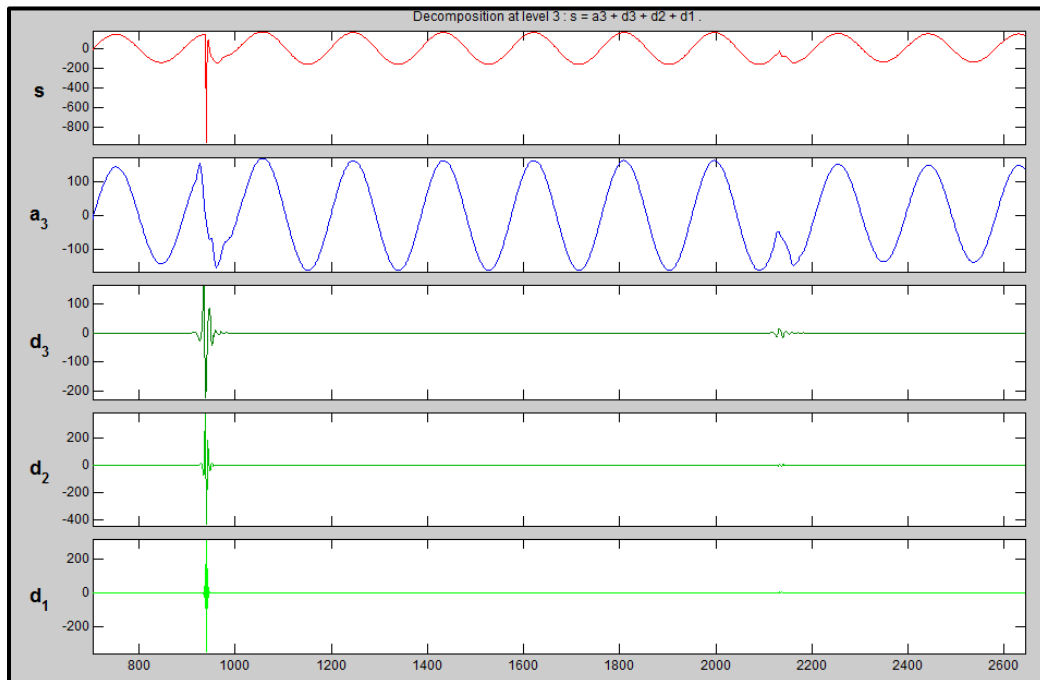
(b) Current I_7 (phase c) .

BUS 7 phase 'c' Voltage(top)

BUS7 phase 'c' Current (bottom)

Voltage(V) & Current (I) MEASUREMENT at Bus 7 for Phase C after applying (L-G) fault .

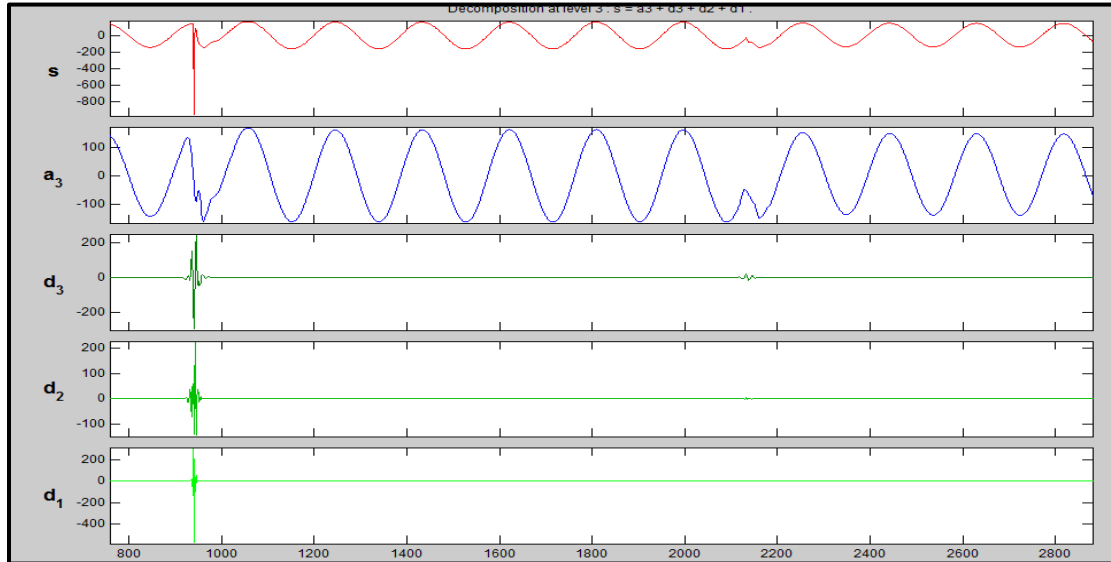
Analyzing **Ic 7**: Bus7 (Phase C)current signal using DWT algorithm



*A Pictur of detail and approximate coefficients. With **db4** wavelet (Level 3 Resolution)*

A Picture of detail and approximate coefficients. With **db6** wavelet (Level 3 Resolution)

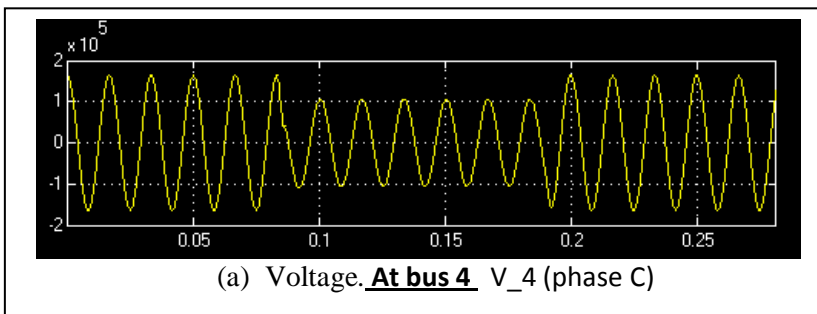
Detail Coefficients Tabulated Also shown



D1	-0.00231	0.031967	-0.01534	-0.00755	0.008196	-0.00199	-0.00134	0.002181	-0.00028	-0.00131
D2	0.078278	0.047352	-0.04066	-0.04062	-0.00153	0.008922	0.020074	0.009089	-0.01387	-0.01132
D3	-0.53414	-0.34899	-0.00371	0.213719	0.316513	0.255918	0.078782	-0.01266	-0.06484	-0.09657

Affect at **BUS4** (phasec) due to LG fault at Bus 7

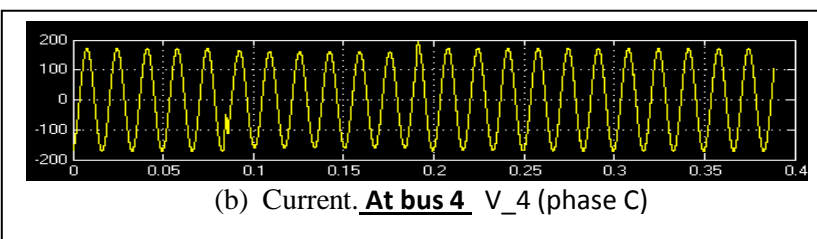
V_{C_4} : Bus 4 Voltage (Phase C)



(a)BUS 4 phase 'c' Voltage(top)

(b)BUS 4 phase 'c' Current
(bottom)

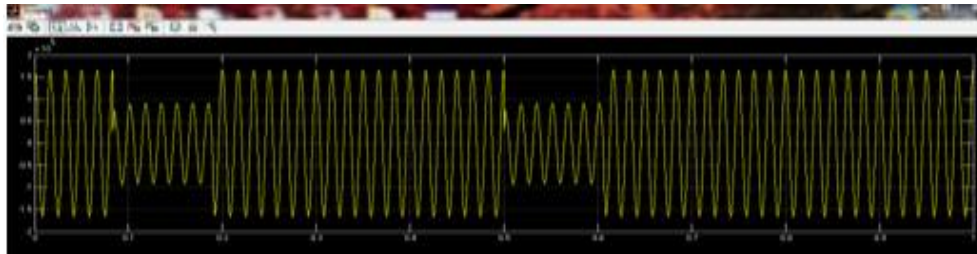
I_{C_4}: Bus4 Current (Phase C):



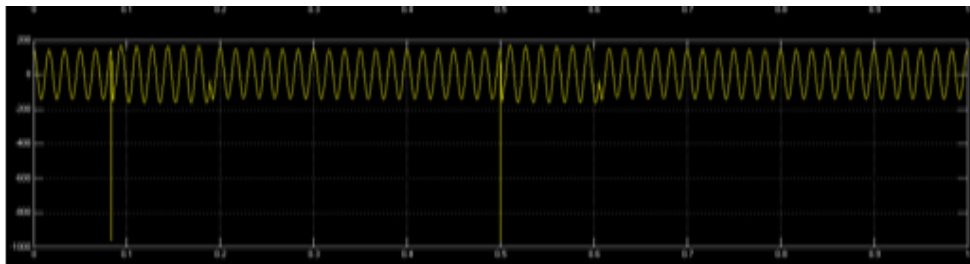
Fault inception at BUS 7 for **0.1s** duration at **t=0.83 s** and **t=0.5s**

- (Fault Impedance **Z_f=100 ohm**)

Voltage(V) & Current (I) MEASUREMENT at Phase C after applying (L-G) fault .



(a) Voltage. At bus 7 V_7 (phase C)



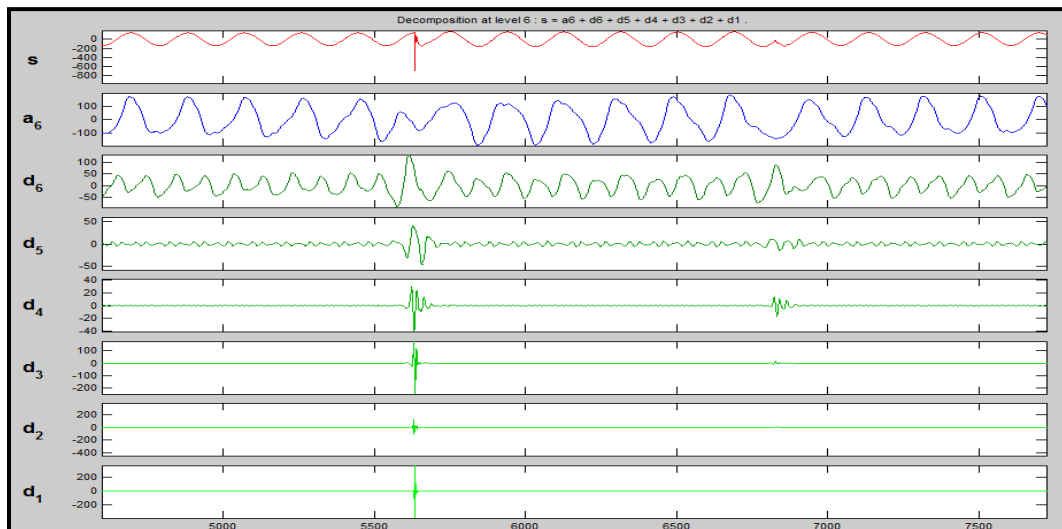
(b) Current. At bus 7 V_7 (phase C)

(a)BUS 7 phase 'c'
Voltage(top)

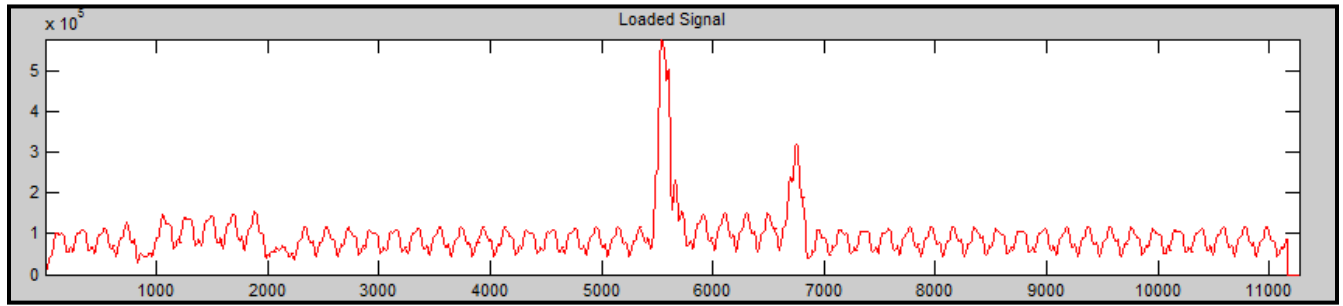
(b)BUS7 phase 'c' Current
(bottom)

Next We perform DWT Algorithm on the measured V-I Samples at BUS 7 and check for transients

.Analyzing Ic 7: Bus7 (Phase C)current signal using DWT algorithm (DB4 –LEVEL 6)



2) Detail Spectrum Energy (DSE) Analysis (\dot{E}_i) (fast rising energies indicating fault)



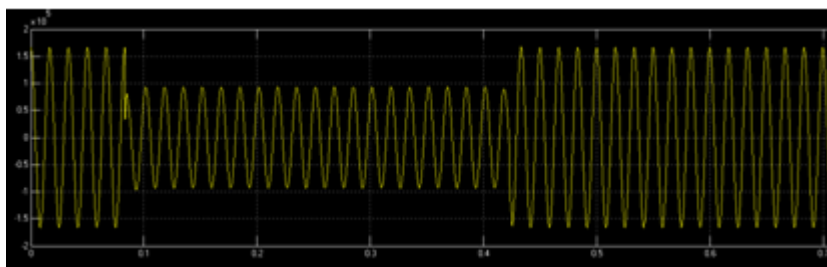
Detail coefficients d1,d2,d3,d4,d5,d6 (from top row to bottom repectively)

Detail Coeffients Tabulated Db4 Level-6

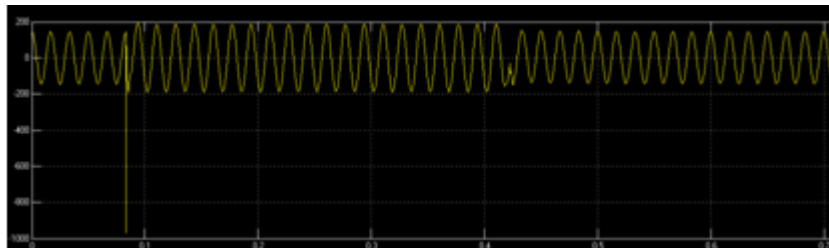
0.0041	-0.0026	-0.0021	0.0027	7.7948e-04	-0.0016	0.0013	5.8213e-04
-0.0153	-0.0075	0.0235	0.0199	-0.0161	-0.0228	-0.0084	0.0018
0.1097	0.0157	-0.1377	-0.2024	-0.1668	-0.1224	-0.0315	0.0220
-0.2635	-0.2294	-0.1043	-0.0222	0.0104	0.0973	0.2097	0.2604
-0.0498	-0.6362	-1.2320	-1.9369	-2.7589	-3.6261	-4.5624	-5.1751
33.2790	34.0943	34.9056	35.2374	35.0544	34.6793	33.9971	33.8038

5.2) LINE TO LINE (L-L)LIF($Z_f=100\Omega$) FAULTS

- Fault inception at BUS 7 for 0.1s duration at $t=0.83s$
- PHASE B –PHASE C (LL FAULT)

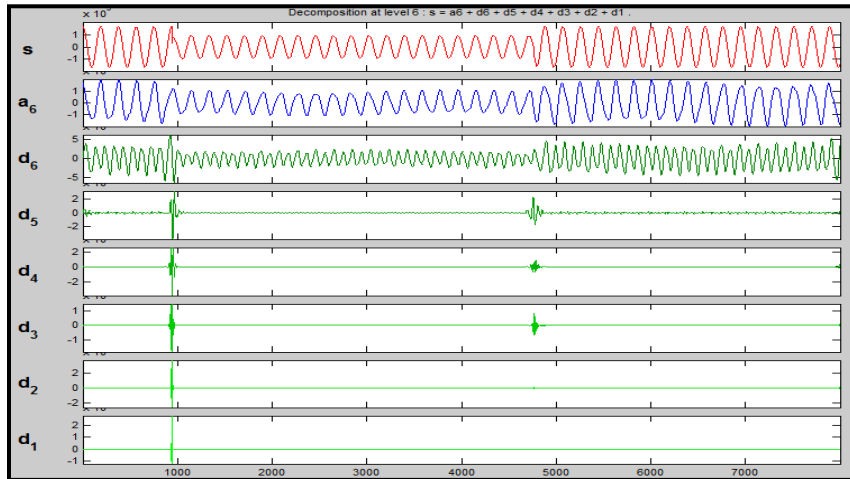


(a)Voltage. At bus 7 V_7 (phase C)



(b)Current. At bus 7 V_7 (phase C)

Voltage V_C_BUS7 DWT With db6 upto level 6 resolution



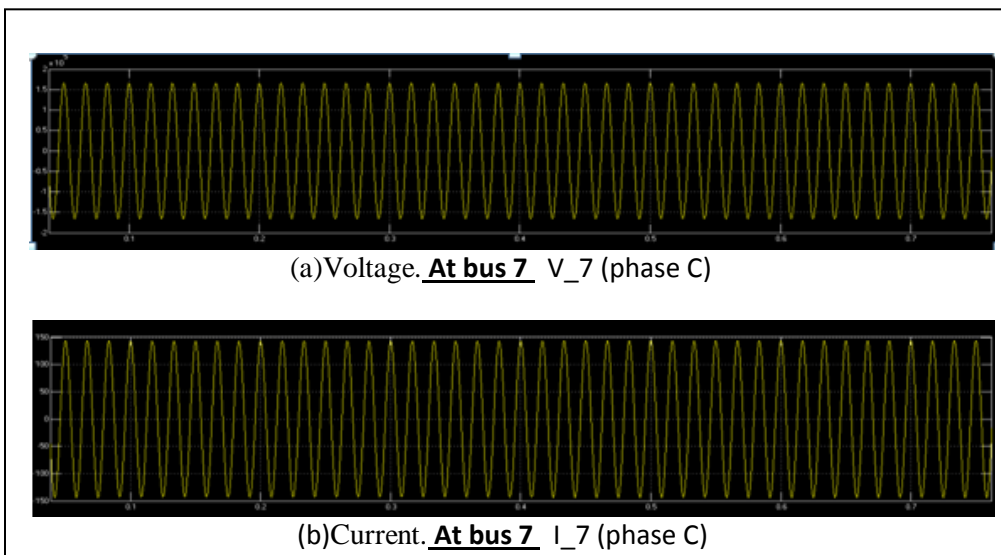
d1	-2.110131	1.537147	-0.31409	-2.20972	3.196085	0.430205	-3.20844	2.298648
d2	2.234167	4.146507	3.639893	-0.32083	-1.91511	-2.01354	-0.29779	2.056974
d3	-143.0151	-148.937	-71.9671	31.40218	116.5752	165.3278	124.909	36.7742
d4	523.3977	637.7481	650.7121	606.4351	548.2853	461.1757	360.0446	245.9303
d5	4784.388	4892.193	4947.383	4972.394	4979.601	4992.224	5043.047	5094.227
d6	19125.99	20564.18	21996.41	23404.14	24767.08	26079.34	27327.09	28516.97

Detail coefficients
d1,d2,d3,d4,d5,d6

LINE TO GROUND (L-G) LIF FAULTS

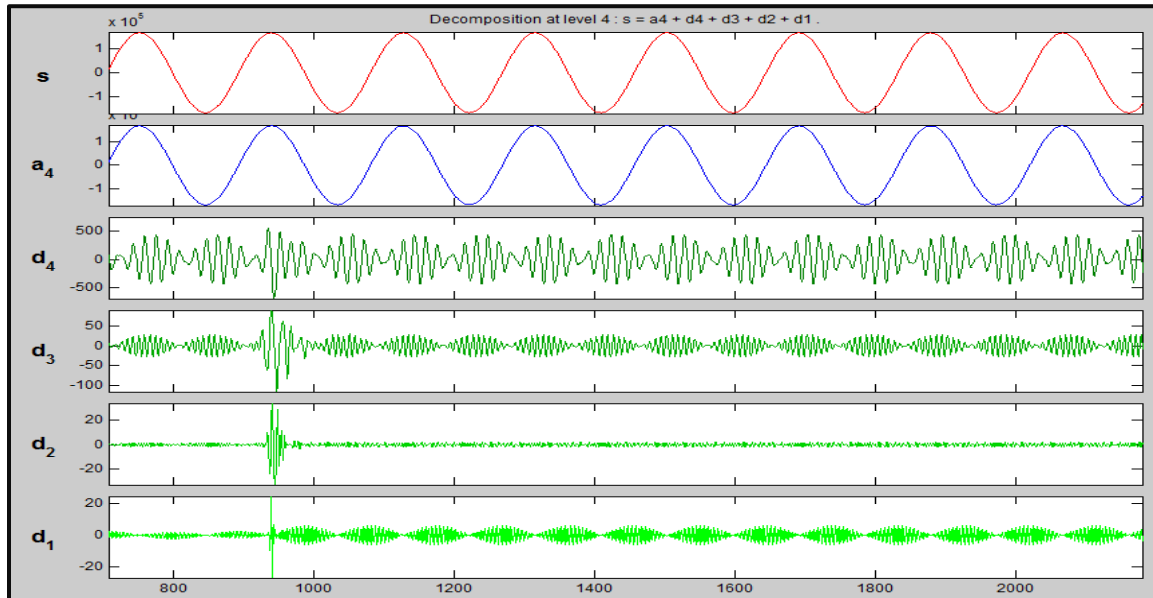
- Fault inception at BUS 7 for 0.1s duration at $t=0.83s$
- Fault Impedance $Z_f=100000$ ohm(100kohm)

Voltage(V) & Current (I) MEASUREMENT at Bus 7 for Phase C after applying (L-G) fault .



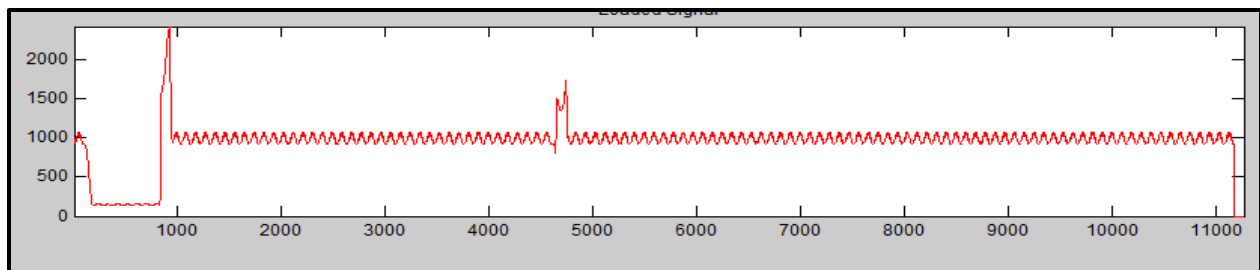
Transients hard to see and detect by normal protective relays.

A Picture of detail and approximate coefficients. With **db4** wavelet (Level 4 Resolution)



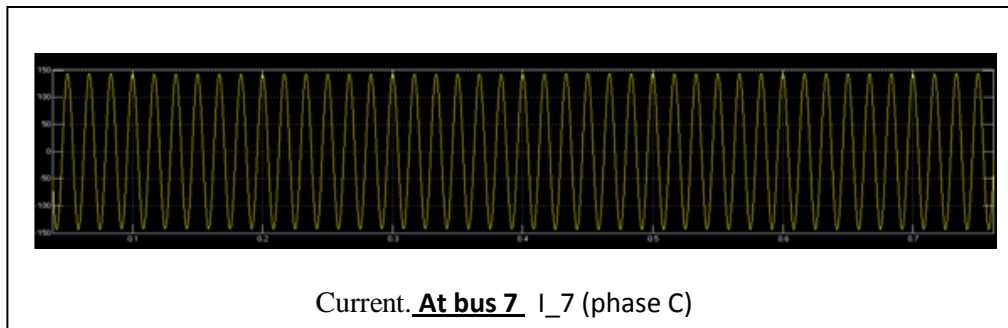
Detail Spectrum Energy (DSE) Analysis

(fast rising energies indicating fault) ($\dot{\epsilon}_v$ for V_{c_7})

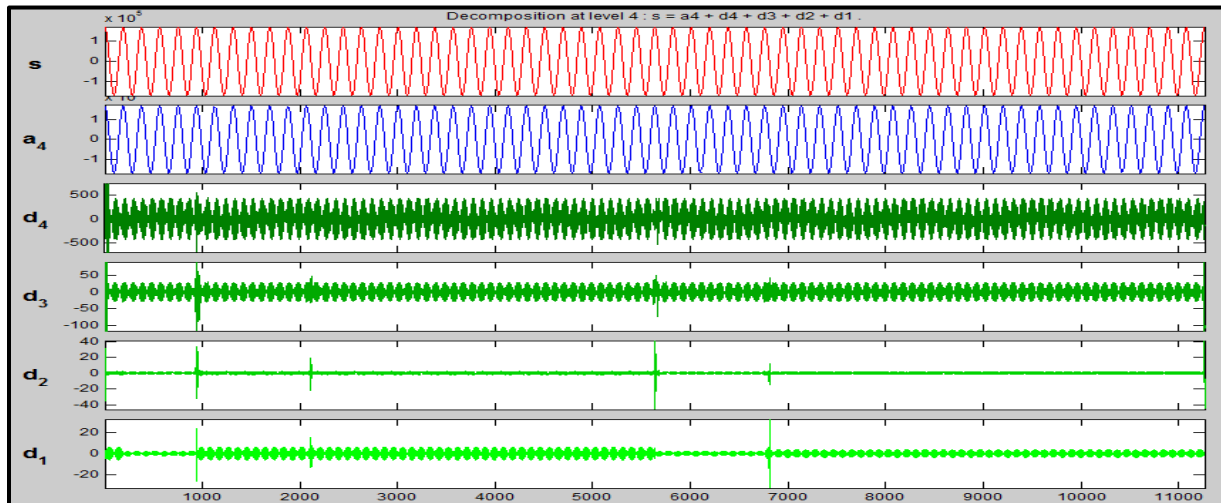


(1.) Fault inception at BUS 7 for 0.1s duration at $t=0.083s$ and $t=0.5$ sec

- Fault Impedance $Z_f=100000$ ohm(100kohm)
- Current (I-bottom) MEASUREMENT at Bus 7 for Phase C after applying (L-G) fault .

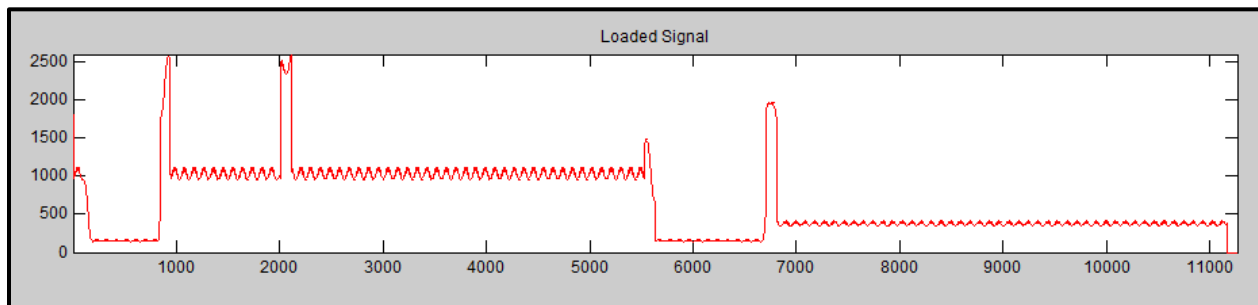


*A Picture of detail and approximate coefficients. With **db4** wavelet (Level 4 Resolution)*



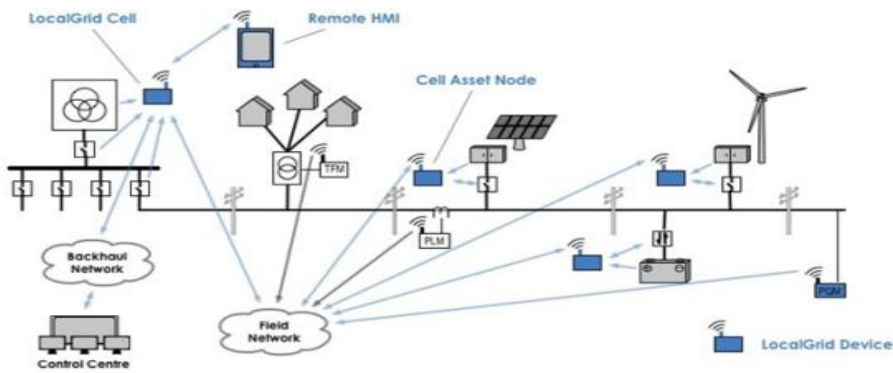
Detail Spectrum Energy (DSE) Analysis

(fast rising energies indicating HIF fault) ($\dot{\epsilon}_v$ for V_{c_7})



The voltage and current at the secondary side of the main transformer near the PCC are available. PT and CT are generally installed at the secondary side of the main transformer. The levels of fault voltage and current are reduced for the further usage of FPGA chip .Now this is the core of an intelligent device. It can carry out the fault detection ,identification or location

algorithms on monitored samples as well as establish a multi-agent system through communication between the intelligent devices,



A Smart Grid Multi-Agent system

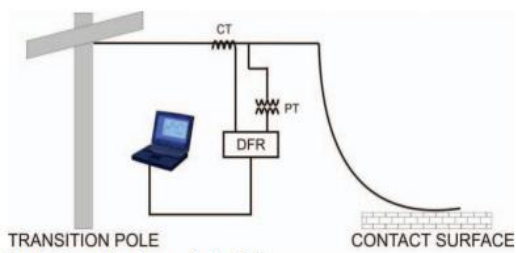
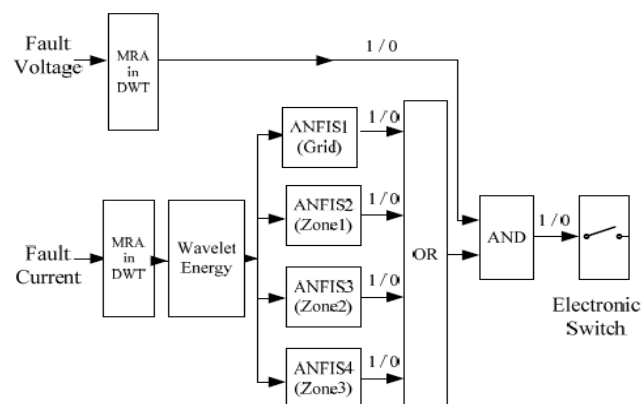


Fig. 4. Connection diagram for the DFR.

DWT FILTER SIMULATION USING FIR Filters in Verilog HDL



3.5. Real-Time Digital Simulation and FPGA Implementation

SIMULATION for filter outputs.

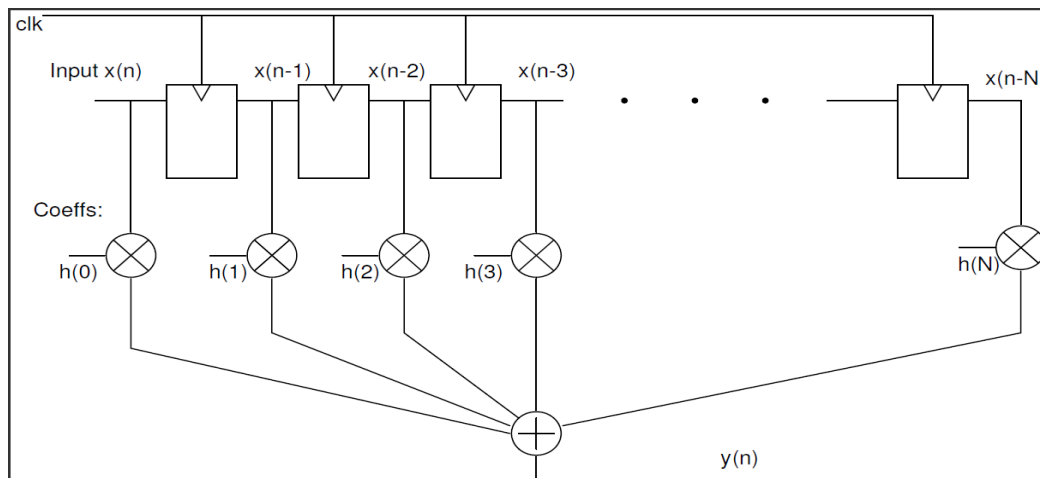
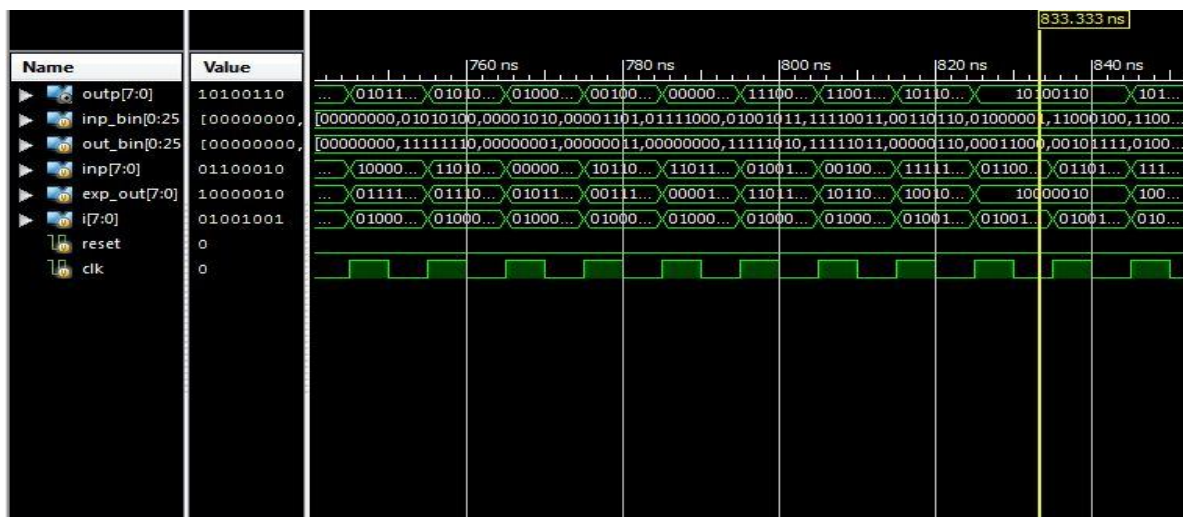
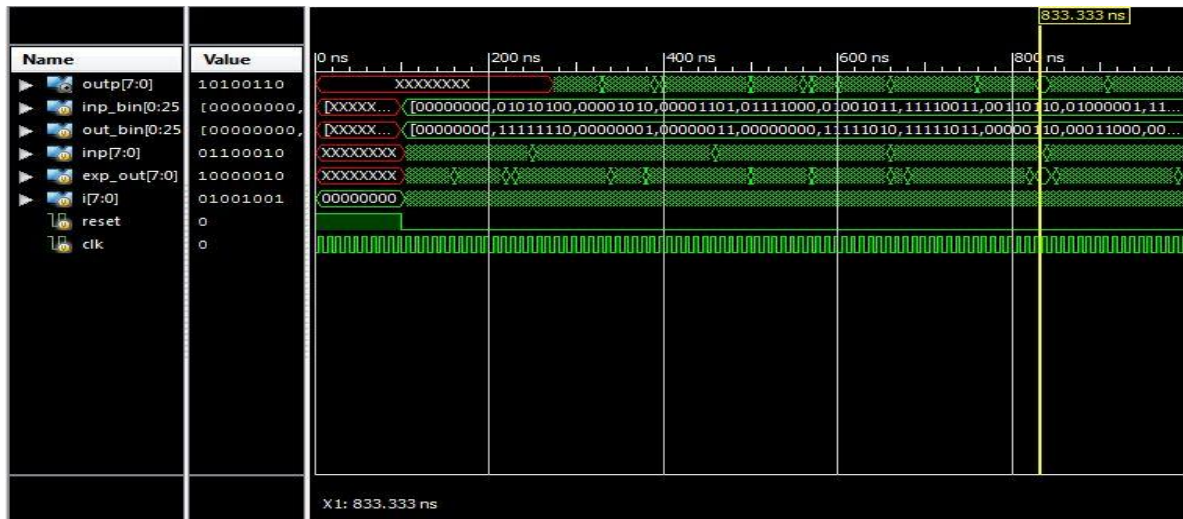


Fig. shows Filter structure implemented with shift registers and booth multipliers.

CHAPTER 6:

SUMMARY:

A transient based approach , Discrete Wavelet Transform (DWT) was used for HIF detection and fault diagnosis on smart (multi-agent) distribution networks and transmission grid networks.

This work utilizes the detail coefficients at different resolutions of the fault currents and voltages and the sum of the squared detail coefficients (DSE) of the fault current to activate the electronic switch to open once a High impedance fault occurs in the grid. All wavelet coefficients are computed using sampled points of both the voltage and current sampled at 40 khz. The DWT is able to detect changes of instantaneous voltage/current by using the detailed coefficients obtained at their corresponding scales ($j = 1, 2, 3, 4, 5, \dots$). The HIF detection step is based on the identification of fast-risings in the energy spectrum of detail-wavelet coefficients while the HIF location approach performs a post-fault processing of the maximum transient energies at strategic areas of the smart grid. As a consequence ,a reduced area is indicated to be inspected and a search sequence is suggested for the maintenance crews.

Traditional effective (rms) values of the fault voltage and current are not suitable to be indicators for detecting the fault occurrence because the faults may occur at zero crossings and also due to lower HIF current values which do not trip the traditional protection devices such as breakers and relays. Although the method is applied off-line, it is also suitable for real-time smart grid applications, since it does not require information regarding the feeder parameters nor about the power system loads.

The proposed algorithm can be implemented on hardware easily, being applicable in any DN, provided that there are available interconnected monitoring points throughout the system and also on TN provided voltages and currents are scaled down significantly by monitoring intelligent devices through appropriate A-to-D conversions.

CONCLUSION:

The algorithm was evaluated through MATLAB simulations of HIF, LG, L-L cases in a WSCC 9-BUS Transmission and Distribution networks. Emanuel HIF model, a well-known HIF model was implemented. The presented results attest that the proposed method is efficient and quite reliable. In all analyzed scenarios, the HIF and LIF was detected and a way to reduce the disturbance search field by setting threshold values was discussed. Finally, one can conclude that the proposed approach may be easily embedded into smart grid devices in order to provide real-time diagnoses of HIFs on smart DNs.

Future Work

The DWT filters banks can be implemented on FPGA Hardware (online implementation) and tested for obtaining different level detail coefficients and Detail Energy values. The results generated can be checked with offline simulations for correctness. After fault detection and estimating fault type, now Fault location by DWT algorithm can also be studied and implemented by making use of smart grid communication channels monitoring grid voltages and currents at strategic points.

The proposed approach for fault detection may be easily embedded into smart grid devices in order to provide real-time diagnoses of HIFs on smart DNs.

Appendix

Flow Charts :

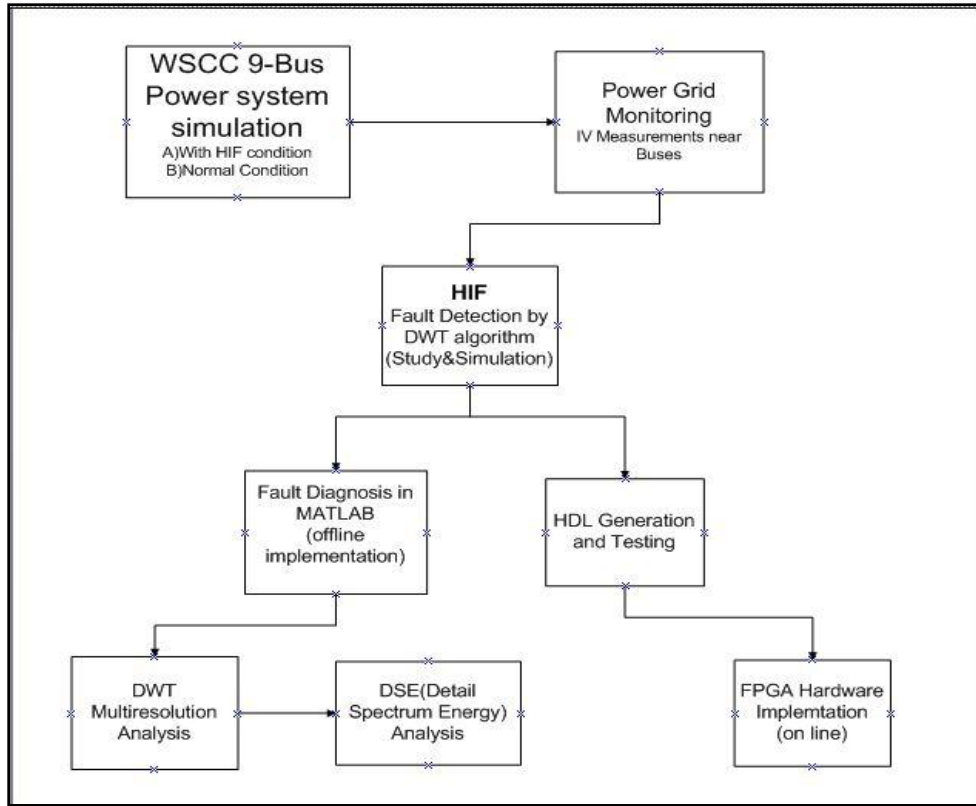
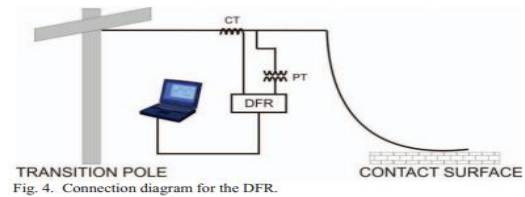
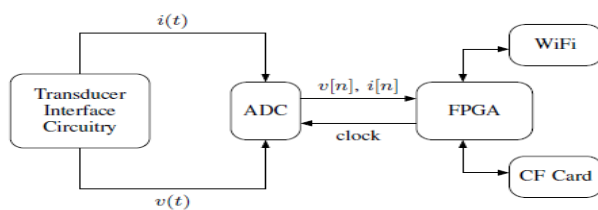
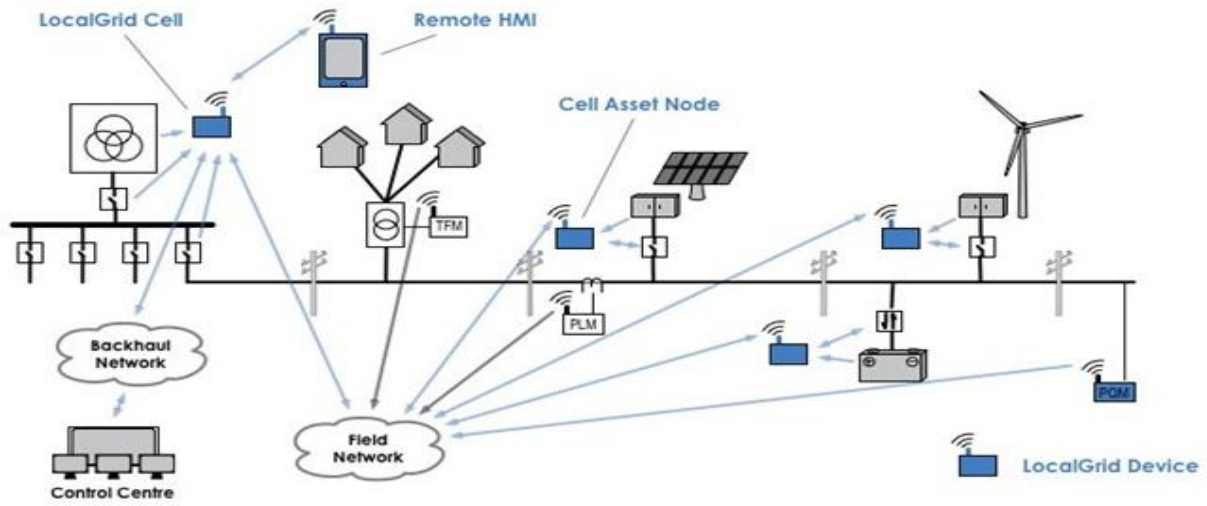


Figure: Summary of the process flow carried out

Experimental Setup : Intelligent devices IN GRIDS.





A Smart Grid Multi-Agent system



g. 5. Photograph of a HIF in dry grass.

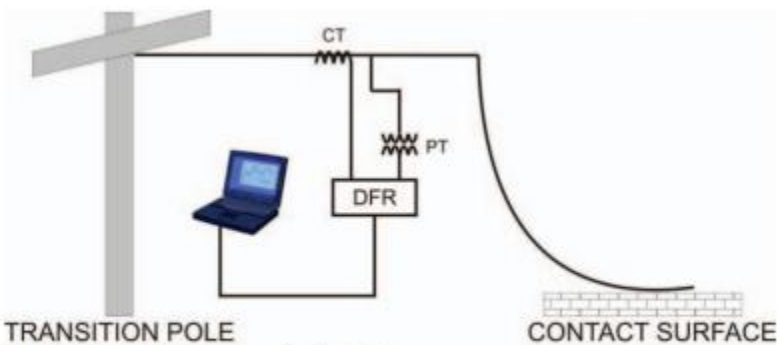


Fig. 4. Connection diagram for the DFR.

References:

- 1) "A Transient Based Approach to Diagnose High Impedance Faults on Smart Distribution Networks" F. V. Lopes, Student Member, IEEE, W. C. Santos, Student Member, IEEE, D. Fernandes Jr., Member, IEEE, W. L. A. Neves, Member, IEEE, N. S. D. Brito, Member, IEEE, B. A. Souza, Senior Member, IEEE
- 2) "High Impedance Fault Detection and Discrimination Using a Wavelet Packet Transform-Based Algorithm " Arash Mahari , Heresh Seyedi
- 3) "Fault Detection and Location by Static Switches in Microgrids Using Wavelet Transform and Adaptive Network-Based Fuzzy Inference System" Ying-Yi Hong 1,*, Yan-Hung Wei 1, Yung-Ruei Chang 2, Yih-Der Lee 2 and Pang-Wei Liu 2
- 4) "Increasing Power Service Reliability and Energy Security With MicroGrids"
- 5) S. Santoso, E. Powers, W. Grady, and P. Hofmann, "Power quality assessment via wavelet transform analysis,"
- 6) A.-R. Sedighi, M.-R. Haghifam, O. Malik, and M.-H. Ghassemian, "High impedance fault detection based on wavelet transform and statistical pattern recognition,".
- 7) J. Liu and P. Pillay, "An insight into power quality disturbances using wavelet multiresolution analysis," .
- 8) Wavelet Toolbox Computation Visualization Programming User's Guide Version 1 Michel Misiti ,Yves Misiti Georges Oppenheim, Jean-Michel Poggi.
- 9) Modeling and Experimental Verification of High Impedance Arcing Fault in Medium Voltage Networks Nagy I. Elkalashy, Matti Lehtonen
- 10) Numerical simulation and analytical model of electrical arc impedance in the transient processes Nenad MARKOVIĆ¹, Slobodan BJELIĆ², Jeroslav ŽIVANIĆ³, Uroš JAKŠIĆ⁴.
- 11) *A Tutorial of the Wavelet Transform by Chun-Lin, Liu*
- 12) Link for fourier transform "<http://www.thefouriertransform.com/>"
- 13) "Transient Energy and its Impact on Transmission Line Faults" Mamta Patel and R. N. Patel.
- 14) "Wavelet Transform Approach to High Impedance Fault Detection in MV Networks" Marek Michalik, Waldemar Rebizant, Mirosław Lukowicz, Seung-Jae Lee, Sang-Hee Kang.
- 15) "High Impedance Fault Detection Technology" Report of PSRC Working Group D15 March 1, 1996 John Tengdin, Chairman, Ron Westfall, Vice Chairman, Kevin Stephan, Secretary Members: M. Adamiak, J. Angel, J. Benton, S. Borlase, S. Boutilier, M. Carpenter, P. Carroll, A. Darlington, D. Dawson, P. Drum, G. Fenner, F. Galvan, M. Gordon, R. Hoad, D. Hemming, J. Huddleston, D. Jamison, T. Kendrew, E. Krizauskas, J. Linders, J. McConnell, M. McDonald, J. Murphy, G. Nail, T. Napikoski, R. Patterson, M. Pratap, R. Reedy, D. Russell, E. Sage, D. Shroff, D. Staszkesky, W. Strang, C. Sufana, B. Tyska, J. Waldron, C. Wester, T. Wiedman, P. Winston, J. Zipp
- 16) "Wavelet based fault detection and classification" Kulkarnisakikekar Smanth Sudhir & R.P.Hasab
- 17) Simulation of High Impedance Ground Fault In Electrical Power Distribution Systems A. R. Sedighi, Member, IEEE, and M. R. Haghifam, Senior Member, IEEE

